

**Geosciences Research Program ER-15**  
**OFFICE OF BASIC ENERGY SCIENCES**

**Reactivity and Mobility of Geologic  
Fluids:  
Constraints from Inorganic  
Geochemistry**

January 29 & 30, 1996  
Oak Ridge, Tennessee

Prepared by  
Oak Ridge National Laboratory

Managed by Lockheed Martin Energy Research Corp.  
for the U.S. DEPARTMENT OF ENERGY under contract DE-ACO5-96OR22464

## FOREWARD

The Geosciences Research Symposium "Reactivity and Mobility of Geologic Fluids: Constraints from Inorganic Geochemistry" is the second of a series of short, topically focused meetings for principal investigators to give presentations and engage in discussions of their BES/Geosciences-supported research on themes of common interest. As the theme of this symposium is central to much of the BES/Geosciences-supported research at Oak Ridge National Laboratory, Dr. Dave Wesolowski, the Geosciences Research Program coordinator, generously agreed to host the meeting in Oak Ridge and arrange for tours of his Geochemistry Group laboratory facilities on site. The meetings provide an opportunity for the investigators to be recognized for outstanding research contributions, one each from a DOE Laboratory project, and from a University project. To help in selecting those to be honored, we are fortunate to have with us as guest session co-chairs Professors Hubert Barnes, Penn State; Thure Cerling, Utah State; Robert Clayton, University of Chicago; and Dr. Jim Hays, recently retired from the directorship of NSF's Earth Sciences Division; who join our Principal Investigator co-chairs Drs. Bill Casey, UC Davis; Mike Murrell, LANL; Jack Sharp, University of Texas; and Ed Stolper, Caltech. For their efforts on behalf of the investigators, I thank them all. We are looking forward to an outstanding series of presentations and discussions.

William C. Luth, Manager  
Geosciences Research Program  
Office of Basic Energy Sciences  
U. S. Department of Energy

## TABLE OF CONTENTS

Agenda	3
Abstracts (listed alphabetically by speaker's name)	7
Attendees	41

## PROGRAM

### Reactivity and Mobility of Geologic Fluids: Constraints from Inorganic Geochemistry

Oak Ridge, Tennessee  
January 29-30, 1996

#### **Sunday, January 28, 1996**

7:00 - 9:00 PM                      Registration

#### **Monday, January 29, 1996**

7:30 - 8:30                          Registration: Coffee/Pastries

#### **ISOTOPIC TRACERS OF FLUID FLOW I**

Chairpersons: James Hays, Michael Murrell

8:40                      D. J. DePaolo                      University of California, Berkeley  
*"Radiogenic Isotope Studies of Reactive Transport in Groundwater"*

9:05                      B. M. Kennedy                      Lawrence Berkeley National Laboratory  
*"The Composition of Noble Gases in Fluids Associated with the San Andreas and Companion Faults"*

9:30                      N. Thonnard                      University of Tennessee  
*"Development of <sup>81</sup>Kr and <sup>85</sup>Kr Analyses for use as Groundwater Tracers"*

9:55                      BREAK

10:10                      M. T. Murrell                      Los Alamos National Laboratory  
*"Magmatic and Aqueous Fluids: Constraints from U-series Measurements"*

10:35                      A. N. Halliday                      University of Michigan  
*"Crustal Fluid Flow and MC-ICPMS"*

11:00                      LUNCH

## FUNDAMENTAL THERMOCHEMICAL AND TRANSPORT PROPERTIES

Chairpersons: Hubert Barnes, William Casey

- 1:00            R. J. Bodnar                            Virginia Tech  
*“Experimental Studies of PVTX Properties of Fluids”*
- 1:25            J. G. Blencoe                                    Oak Ridge National Laboratory  
*“Thermodynamic Mixing Properties of C-O-H-N Fluids”*
- 1:50            J. A. Rard                                        Lawrence Livermore National Laboratory  
*“Recent Thermodynamic and Transport Property Measurements for Various Aqueous Geochemical Systems”*
- 2:15            R. H. Wood                                      University of Delaware  
*“Toward an Equation of State for Nonelectrolytes in Water”*
- 2:40            W. H. Casey                                      University of California, Davis  
*“Excess Gibbs Energies of Mixing of Metal Carbonate Solutions”*
- 3:05            A. Navrotsky                                    Princeton University  
*“Thermodynamics of Carbonates”*
- 3:30            BREAK
- 3:45            D. J. Wesolowski                                Oak Ridge National Laboratory  
*“Hydrogen-Electrode Potentiometric Studies of Aqueous Geochemical Processes”*
- 4:10            D. R. Cole                                        Oak Ridge National Laboratory  
*“Stable Isotope Exchange Equilibria and Kinetics”*
- 4:35            J. Horita     Oak Ridge National Laboratory  
*“Salt Effects on Stable Isotope Partitioning”*
- 5:00            M. C. Johnson                                   West Point Military Academy  
*“Brine Mobility in Matrices with Retrograde Solubility”*
- 5:25            J. Brenan                                         Lawrence Livermore National Laboratory  
*“Mineral-Fluid Trace Element Partitioning at Elevated P and T”*
- 5:50            S. Brantley                                        Pennsylvania State  
*“Investigations into the Surface Chemistry of Dissolving Feldspar”*

Tuesday, January 30, 1996

7:30 - 8:10                      Coffee/Pastries

## **GEOCHEMICAL TRANSPORT PROCESSES: DYNAMICS AND MODELLING**

Chairpersons: Thure Cerling, John Sharp

8:10                      P. K. Swart                      University of Miami  
*"Geochemical Evidence for Fluid Flow in Carbonate Platforms"*

8:35                      J. Bahr                      University of Wisconsin  
*"Coupled Modeling of Fluid and Heat Flow in the Bahama Bank"*

9:00                      J. M. Sharp                      University of Texas  
*"Fluid and Heat Flow in the Gulf of Mexico Basin, South Texas"*

9:25                      R. D. Elmore                      University of Oklahoma  
*"Origin and Timing of Fluid Flow Events in a Fault Zone, Southwest England:  
Paleomagnetic and Geochemical Results"*

9:50                      BREAK

10:15                      R. Berner                      Yale University  
*"Field Experiment on the Role of Plants in Weathering"*

10:40                      C.-F. Tsang                      Lawrence Berkeley National Laboratory  
*"Scientific Cooperation with Russian Scientists on Contaminant Transport"*

11:05                      J. P. Evans                      Utah State University  
*"Insights into Fault-Fluid Interactions Based on Whole Rock Geochemistry"*

11:30                      R. Glass                      Sandia National Laboratory  
*"Two Phase Flow in Fractures"*

11:55                      LUNCH

## ISOTOPIC TRACERS OF FLUID FLOW II

Chairpersons: Robert Clayton, Edward Stolper

1:30 E. M. Stolper California Institute of Technology  
*"Case Studies of Stable Isotopes in Igneous Petrology"*

1:55 J. Valley University of Wisconsin  
*"Contrasting Mechanisms of Fluid/Rock Exchange"*

2:20 D. R. Bell Geophysical Laboratory  
*"Isotopic Studies of Mantle Hydrogen"*

2:45 R. L. Hervig Arizona State University  
*"Fluid Compositional Changes in North Sea Reservoirs Recorded by O-Isotopic Zoning in Quartz Overgrowths"*

3:10 BREAK

3:25 G. J. Wasserburg California Institute of Technology  
*"The Transport of U, Th, Ir, and Re in Oxidizing/Reducing Environments from the Continents to the Sea"*

3:50 G. N. Hanson SUNY, Stony Brook  
*"U-Pb Dating of Paleocaliche"*

4:15 L. R. Riciputi Oak Ridge National Laboratory  
*"Stable Isotope Studies by Ion Microprobe"*

4:40 K. D. McKeegan University of California, Los Angeles  
*"Development of Monazite as a Prograde Thermochronometer: Diffusion Experiments and In-Situ Th-Pb Dating"*

5:05 T. M. Harrison University of California, Los Angeles  
*"K-feldspar Thermochronometry"*

5:30 DISCUSSION

6:30 RECEPTION IN THE POOL AREA

7:00 DINNER

## **Coupled Modeling of Fluid and Heat Flow in the Bahama Bank.**

J. M. Bahr and S. Rashad, Department of Geology and Geophysics, University of Wisconsin at Madison; G. Eberli and P. Swart, Marine Geology and Geophysics Department, University of Miami

Mechanisms that have been proposed as driving forces for fluid circulation in carbonate banks include (1) reflux of dense water that results from evaporation in shallow water above the bank, (2) circulation associated with a fresh water lens that develops as the result of precipitation recharge on an island, (3) sea-level differences resulting from large scale ocean currents, which generate a hydraulic gradient across the bank, and (4) thermal convection generated by the natural geothermal flux.

The objective of our numerical modeling is to provide a quantitative assessment of the potential interactions between these driving forces and to evaluate the effects of bank scale permeability variations on the resulting fluid circulation patterns and steady-state temperature distributions. We have used the USGS finite difference code HST3D to solve coupled equations for fluid flow, heat flow, and solute transport. The simulation region represents a two-dimensional cross section, which is roughly patterned on a section through North Andros Island on the Great Bahama Bank. The section extends to a depth of 3 km and is approximately 170 km wide. Boundary conditions include a specified heat flux through the lower boundary, a specified fluid flux of fresh water through the upper boundary in the region of North Andros Island, and specified pressures, temperatures, and salinities along the top and sides of the bank that are in contact with sea water.

The model includes three major permeability zones: (1) quaternary carbonate across the top of the bank, which is known to be cavernous and very permeable, (2) deposits from the former Straits of Andros and the Straits of Florida, and (3) the older Bimini and Andros Banks. Core plug permeabilities from two core holes drilled as part of the Bahamas Drilling Project provide some constraints on permeability of carbonate deposited in the Straits of Florida. Because there are few constraints on permeability of the older bank deposits, this parameter was varied in sensitivity analyses.

Simulation results indicate that, for the range of parameters and boundary conditions investigated, geothermal flux is the dominant driving force for bank scale fluid circulation. For a homogeneous permeability distribution, the geothermal flux induces numerous small circulation cells. Variations in permeability due to the major zones listed above lead to larger scale "Kohout" convection cells, with cool ocean water entering the bank along the deeper margins of the bank, being warmed during transport through the bank, and exiting at higher elevations. Sea-level differences of up to 0.6 m do not generate cross-bank flow. Evaporative reflux and fresh-water recharge have local effects on salinity and flow directions, but the bank scale circulation patterns and steady-state temperature distributions are relatively insensitive to these processes. Temperature distributions, particularly along the steep margins of the bank, are sensitive to permeability anisotropy and to permeability contrasts between the straits and bank deposits.



## Isotopic Studies of Mantle Hydrogen.

D. R. Bell and T. C. Hoering, Geophysical Laboratory, Carnegie Institution of Washington

D/H ratios are, in principle, useful in characterizing reservoirs of mantle hydrogen and as tracers of volatile transfer processes in Earth's interior. In practice, however, surface processes such as contamination and degassing, which may alter the primary D/H ratio, complicate the interpretation of isotopic measurements on mantle-derived H. Although there are indications<sup>1-3</sup> that water associated with subduction zones and certain chemically enriched basalts is enriched in D relative to "typical" upper mantle water, the extent of isotopic heterogeneity of mantle H remains uncertain. Kaersutitic amphibole megacrysts in alkaline basalts is one of the most widespread sources of mantle water and is therefore potentially useful for large-scale regional studies of D/H variation. However, D/H ratios of these amphiboles vary widely (from +8 to -113‰),<sup>4</sup> even in samples from the same locality, so that this potential has yet to be realized.

In order to investigate the origin of this variability and to explore the possibility that primary mantle D/H ratios may be deduced from these amphiboles, we analyzed the D/H ratios and chemical compositions of a suite of 17 kaersutitic amphiboles from Dish Hill, California. This work contrasts with previous studies in which sampling is widespread but representatives from any given locality are few. Samples were collected from a restricted area on the southern flank of the volcanic center and are associated with the basal volcanic breccia.<sup>5</sup> Fourteen of the samples were large single crystals or crystal fragments (megacrysts, 0.4 to 30.0 grams), believed to derive from pegmatitic veins crystallized from melts in the mantle. Two were coarse-grained intergrowths of amphibole with olivine and spinel, and one was a thin (2 mm) selvage on a peridotite xenolith.

The samples range in MG #  $\{=100 \text{ Mg}/(\text{Mg} + \text{Total Fe})\}$  from 55 to 85, with the polymineralic intergrowths having highest Mg #'s. In the megacryst samples, the abundances of all elements analyzed by electron microprobe vary systematically with Mg#, giving reason to expect concomitant behavior in the primary water content of these samples. The polymineralic and selvage samples are displaced from these trends to varying degrees. Our data confirm a general systematic behavior for H: 12 of the 14 megacrysts are displaced from this trend to significantly lower H<sub>2</sub>O contents of 0.59 and 0.04 wt. %, respectively.  $\delta\text{D}$  of the former sample is -9‰, while the latter provided insufficient H for isotopic analysis. The polymineralic and selvage samples have H<sub>2</sub>O contents of 1.08 to 1.15 wt. %, with  $\delta\text{D}$  from -37 to -45‰.

The uniformity of these results suggests that primary H content and isotopic composition is preserved in most of these samples. Low H contents of the two anomalous megacrysts and the high D/H ratio are probably the product of dehydrogenation-oxidation.<sup>6,7</sup> It is likely that this process occurred during transport and eruption as there are no other indications of unusual chemistry in these samples. The high degree of uniformity observed, relative to similar previous studies, may be due to local volcanology.<sup>6</sup> Within the limits of current uncertainty of the relevant D/H fractionations, the mean "undisturbed"  $\delta\text{D}$  of -46‰ for the amphiboles could reflect equilibrium with water, occurring as OH groups in a melt, of  $\delta\text{D}$  near -70‰, typical of depleted upper mantle. The MORB-like affinity of these megacrysts is indicated by their Sr isotope compositions<sup>8</sup>.

We conclude that H-isotope information, useful for global systematic studies, can be extracted from mantle-derived amphiboles, providing the appropriate consideration is given to petrographic features, petrologic affinity, and volcanological history of the samples.

## References:

1. Poreda, R. 1985. *EPSL* **73**, 244-254.
2. Poreda, R., et al. 1986. *EPSL* **78**, 1-17.
3. Dobson, P. F. and O'Neil, J. R. 1987. *EPSL* **82**, 75-86.
4. Boettcher, A. L. and O'Neil, J. R. 1980. *Am. J. Sci.* **280A**, 594-621.
5. Wilshire, H. G. and Nielsen-Pike, J. E. 1986. In *GSA Guidebook, Southern California Field Trips* **15** (P. L. Ehlig, ed.), 9-11.
6. Aoki, K. 1963. *J. Petrol.* **4**, 198-210.
7. Dyar, M. D., et al. 1992. *Geology* **20**, 565-568.
8. Basu, A. R. and Murthy, V. R. 1977. *Geology* **5**, 365-368.

### **Field Experiment on the Role of Plants in Weathering.**

R. A. Bemer, Department of Geology and Geophysics, Yale University, and M. F. Cochran, Department of Geological Sciences, University of Kentucky

A major control on atmospheric CO<sub>2</sub> over long geological time scales is the chemical weathering of silicate minerals, and an important factor in this weathering is the role played by higher plants. Our objective is to determine the quantitative effect of trees and other vascular plants in accelerating the weathering rate of silicates by performing controlled experiments under natural field conditions.

Dissolved element concentrations in throughfall and drain waters for small (60 m<sup>2</sup>) vegetated and unvegetated plots are presently being determined as part of an ongoing ecological experiment at the Hubbard Brook Experimental Forest Station in New Hampshire. Three plots are being investigated: one that was planted with red pine in 1983, one planted with two species of grass (also in 1983), and a control containing only mosses and lichens and kept free of higher plants over the same period. All plots are underlined with an impermeable plastic so that water passing through the plots can be collected at an outlet pipe. By correcting for measured rain and snowmelt inputs, as well as evapotranspiration (by normalizing to Cl), we can determine relative release rates of dissolved species in drainage from each plot. Flow rates are determined at the site, and we are analyzing waters collected over the past 12 years and now being collected weekly for Na<sup>+</sup>, K<sup>+</sup>, Ca<sup>++</sup>, Mg<sup>++</sup>, SO<sub>4</sub><sup>2-</sup>, NO<sub>3</sub><sup>-</sup>, Cl<sup>-</sup>, HCO<sub>3</sub><sup>-</sup>, F<sup>-</sup>, H<sub>4</sub>SiO<sub>4</sub>, and pH. These water chemical results, when combined with data on storage in growing biomass and soil (from the results of other workers), will allow us eventually to obtain overall element release rates from primary minerals via chemical weathering.

We have found a several-fold acceleration of the flux of all dissolved cations from the pine-covered plot relative to the plant-free control. The effect is greatest for Na. Uptake by the growing plants of K, Ca, and Mg causes their release in drainage waters to be less than that for Na, which is much less involved in biological cycling. Silica release rates are also distinctly elevated in the tree-covered plot. Similar results, but with a lesser accelerating effect, are found for the grass-covered plot. The fixation of CO<sub>2</sub> as HCO<sub>3</sub><sup>-</sup> is greatly accelerated under the trees, and to a lesser extent under the grass, in the spring. We hypothesize that this is due to the protection from sulfuric and nitric acid precipitation during the winter by a snow cover and the consequent buildup of alkalinity due to continued silicate weathering by organic and carbonic acids. This "old" water is then gradually flushed out in the spring and replaced by acidic snowmelt. Sulfate and H<sup>+</sup> are enriched in drainage from the tree-covered plot at other times, possibly due to enhanced trapping of sulfuric acid aerosols by pine needles.

## Thermodynamic Mixing Properties of C-O-H-N Fluids at High Pressures and Temperatures.

J. G. Blencoe, J. C. Seitz, L. M. Anovitz\*, and D. B. Joyce\*, Chemical and Analytical Sciences Division, Oak Ridge National Laboratory, and R. J. Bocinar\*, Department of Geological Sciences, Virginia Polytechnic Institute and State Univ.

Fluids composed predominantly of carbon, oxygen, hydrogen, and nitrogen have played a key role in mass and energy transfer processes in the earth's crust. Thus, it is unfortunate that very few reliable data are available on the physicochemical properties of these fluids. We are addressing this problem by obtaining precise and accurate experimental data on the thermodynamics and phase relations of C-O-H-N fluids at 50-2000 bars, 50-700°C. This research (the "C-O-H-N Project") is divided into two distinct but complementary endeavors: a *P-V-T Task* and a *P-T-X Task*. The principal aim of the *P-V-T Task* is to measure the volumetric properties of C-O-H-N fluids. The main goal of the *P-T-X Task* is to determine the activity-composition (*a-X*) relations of aqueous C-O-H-N fluids. The data obtained in these research activities are being combined with suitable literature data to develop new equations of state (EOSs) for binary and multicomponent mixtures of H<sub>2</sub>O, CO<sub>2</sub>, CH<sub>4</sub>, and N<sub>2</sub>.

Volumetric properties of C-O-H-N fluids (*P-V-T Task*): A unique, custom-designed vibrating U-tube densimeter (Blencoe et al., 1996) was used to make >1000 measurements of the *P-V-T* properties of pure CO<sub>2</sub>, pure CH<sub>4</sub>, and binary and ternary CO<sub>2</sub>-CH<sub>4</sub>-N<sub>2</sub> fluids at 100-1000 bars, 50-400°C (Seitz et al., 1992, 1994, 1996a,b; Seitz and Blencoe, 1996). Measured parameters were *P*, *T*, and  $\tau$  (period of vibration). Densities ( $\rho$ ) were determined relative to three reference fluids (He, N<sub>2</sub>, and Ar). Conservative estimates of accuracy are *P*,  $\pm 0.2$  bars; *T*,  $\pm 0.05^\circ\text{C}$ , and  $\rho$ ,  $\pm 0.0005\text{--}0.0010\text{ g/cm}^3$ . Results of this research indicate that (1) excess molar volume ( $V^{\text{ex}}$ ) for binary and ternary CO<sub>2</sub>-bearing mixtures increases sharply near the critical point of CO<sub>2</sub> (31.1°C, 73.6 bars); (2) CO<sub>2</sub>-bearing binary and ternary mixtures exhibit both positive and negative  $V^{\text{ex}}$ ; (3) the *P-V-T* properties of CO<sub>2</sub>-CH<sub>4</sub>-N<sub>2</sub> fluids are inaccurately predicted by published EOSs; and (4) the volumetric properties of ternary CO<sub>2</sub>-CH<sub>4</sub>-N<sub>2</sub> mixtures can be estimated with good accuracy from  $V^{\text{ex}}$  data for the binary mixtures using several different types of geometric projection techniques.

Activity-composition relations of aqueous C-O-H-N Fluids (*P-T-X Task*): More than 100 fluid samples containing H<sub>2</sub>O, an oxygen buffer (Ni-NiO or Co-CoO), and CO<sub>2</sub> or N<sub>2</sub> were reacted in a 2.5" I.D., hydrogen-service internally heated pressure vessel (IHPV) at constant *P*, *T*, and  $f_{\text{H}_2}$ , to determine the *a-X* relations of H<sub>2</sub>O-CO<sub>2</sub> mixtures at 500 bars, 400-700°C (Joyce and Blencoe, 1994; Anovitz et al., in preparation), and the *a-X* relations of H<sub>2</sub>O-N<sub>2</sub> mixtures at 500 bars, 500°C (Anovitz et al., in preparation). During experimentation,  $X_{\text{H}_2\text{O}}$  in each sample either increased or decreased, depending on *P*, *T*,  $f_{\text{O}_2}$  and the  $f_{\text{H}_2}$  established by the Ar-H<sub>2</sub> atmosphere in the IHPV. After quenching, the mass of H<sub>2</sub>O in each sample was determined by converting H<sub>2</sub>O to H<sub>2</sub> in a uranium furnace, and measuring  $P_{\text{H}_2}$  manometrically. Considering all potential sources of error in the experimentation, conservative estimates of uncertainty are  $a_{\text{H}_2\text{O}}$ ,  $\pm 0.003\text{--}0.03$ ; and  $X_{\text{H}_2\text{O}}$ ,  $\pm 0.01$ . Results of this research indicate that (1) H<sub>2</sub>O-CO<sub>2</sub> fluids exhibit continuously positive deviations from Raoult's law behavior at 500 bars, 400-700°C; (2) the modified Redlich-Kwong EOSs developed by Holloway (1977) and Kerrick and Jacobs (1981) fall to provide accurate calculated activities for H<sub>2</sub>O-CO<sub>2</sub> fluids at 500 bars, 400-700°C; and (3) at a given *P* and *T*, H<sub>2</sub>O-N<sub>2</sub> fluids are more nonideal than H<sub>2</sub>O-CO<sub>2</sub> fluids.

## References

- Anovitz, L. M., Blencoe, J. G., Joyce, D. B., and Horita, J., 1996, Precise Measurement of Activity-Composition Relations of  $\text{H}_2\text{O}-\text{N}_2$  and  $\text{H}_2\text{O}-\text{CO}_2$  Fluids at  $500^\circ\text{C}$ , 500 bars (in preparation).
- Blencoe, J. G., Drummond, S. E., Seitz, J. C., and Nesbitt, B. E., 1996, A Vibrating-Tube Densimeter for Fluids at High Pressures and Temperatures, *Int. J. Thermophys.* (in press).
- Joyce, D. B. and Blencoe, J. G., 1994, Excess Molar Free Energies for  $\{x\text{H}_2\text{O} + (1-x)\text{CO}_2\}$  at Temperatures from 673 K to 973 K, at the Pressure 50 MPa, *J. Chem. Thermodyn.* 26, 765-777.
- Seitz, J. C. and Blencoe, J. G., 1996, Volumetric Properties for  $\{(1-x)\text{CO}_2 + x\text{CH}_4\}$ ,  $\{(1-x)\text{CO}_2 + x\text{N}_2\}$ , and  $\{(1-x)\text{CH}_4 + x\text{N}_2\}$  at the Pressures (19.94, 29.94, 39.94, 59.93, 79.93, and 99.93) MPa and the Temperature 673.15 K (in preparation).
- Seitz, J. C., Blencoe, J. G., Joyce, D. B., and Bodnar, R. J., 1992, Excess Molar Volumes for  $\text{CO}_2-\text{CH}_4-\text{N}_2$  Mixtures, *Proc., 7th Int. Symp. on Water-Rock Interaction* (Y. K. Kharaka and A. S. Maest, eds.), Rotterdam: A. A. Balkema, 1025-1028.
- Seitz, J. C., Blencoe, J. G., Joyce, D. B., and Bodnar, R. J., 1994, Volumetric Properties of  $\text{CO}_2-\text{CH}_4-\text{N}_2$  Fluids at  $200^\circ\text{C}$  and 1000 Bars: A Comparison of Equations of State and Experimental Data, *Geochim. Cosmochim. Acta* 58, 1065-1071.
- Seitz, J. C., Blencoe, J. G., and Bodnar, R. J., 1996, Volumetric Properties of  $\{(1-x)\text{CO}_2 + x\text{CH}_4\}$ ,  $\{(1-x)\text{CO}_2 + x\text{N}_2\}$ , and  $\{(1-x)\text{CH}_4 + x\text{N}_2\}$  at the Pressures (9.94, 19.94, 29.94, 39.94, 59.93, 79.93, 99.93) MPa and Temperatures (323.15, 373.15, 473.15, 573.15) K, *J. Chem. Thermodyn.* (in press).
- Seitz, J. C., Blencoe, J. G., and Bodnar, R. J., 1996, Volumetric Properties of  $\{x_1\text{CO}_2 + x_2\text{CH}_4 + (1-x_1-x_2)\text{N}_2\}$  at the Pressures (19.94, 39.94, 59.93, 99.93) MPa and Temperatures (323.15, 373.15, 473.15, 573.15) K, *J. Chem. Thermodyn.* (in press).

## **Experimental Studies of PVTX Properties of Fluids.**

R J Bodnar, Fluids Research Laboratory, Department of Geological Sciences, Virginia Polytechnic Institute and State University

Volumetric (PVTX) properties of fluid systems represent the fundamental information required to calculate thermodynamic properties of fluids. For the past several years, workers in the Fluid Research Laboratory have been conducting experimental studies to determine the PVTX properties of geologically important fluid systems over the range of PTX conditions applicable to energy, industrial, and hazardous waste remediation environments. At the present time, efforts are focused on three related systems:  $\text{H}_2\text{O}$ -NaCl,  $\text{H}_2\text{O}$ - $\text{CO}_2$ -NaCl and  $\text{H}_2\text{O}$ - $\text{CH}_4$ - "hydrocarbons". We (and others) are using the data obtained in these studies to develop equations of state to predict the volumetric properties of these fluids in crustal environments.

The system  $\text{H}_2\text{O}$ -NaCl serves as a model for fluids in terrestrial geothermal systems, in many hydrothermal ore-forming environments, in steam power generation facilities, and in reactors employed in the destruction of hazardous waste using supercritical water oxidation technologies: Experimental studies of the PVTX properties of this important system over the range of PTX conditions appropriate to the above environments have been completed, and an empirical equation describing the physical properties of the system has been developed and tested. This equation allows the phase behavior and densities of  $\text{H}_2\text{O}$ -NaCl fluids to be predicted over a wide range of PTX conditions.

Supercritical water oxidation of hazardous waste often results in production of a high-salinity brine containing the gaseous products of the breakdown of the hazardous materials. The dominant component of the gas is often carbon dioxide, and much effort has been focused on the development of a reaction cycle that permits separation of the more volatile gas from the less volatile aqueous component. Using the system  $\text{H}_2\text{O}$ - $\text{CO}_2$ -NaCl as a model, experiments have been conducted in the PTX applicable to supercritical water oxidation processes to better constrain the phase equilibrium and PVT properties of immiscible fluids in this system. The goal of this work is to identify the range of conditions in which the separation of the more volatile ( $\text{CO}_2$ ) component from the less volatile ( $\text{H}_2\text{O}$ -NaCl) components occurs most effectively.

Preliminary experiments have been conducted to generate methane and higher hydrocarbons (petroleum) *in situ* through hydrous pyrolysis of an immature source rock (New Albany shale). The resulting fluids are then trapped as synthetic fluid inclusions in quartz and other mineral phases at the temperatures and pressures of the experiments. Examination of the synthetic fluid inclusions after the experiment permits identification of phase boundaries (bubble-point/dew-point curves) and mutual solubilities of hydrocarbons and water. These data provide a more complete understanding of the physical and chemical processes associated with the generation and migration of oil and natural gas in the subsurface.

## **Investigations into the Surface Chemistry of Dissolving Feldspar.**

S. L. Brantley, Department of Geosciences, Pennsylvania State University

The inherent difficulty in validating numerical models of fluid, solute, and heat transport in the subsurface requires that multiple data sets be collected and used to "ground-truth" environmental simulations. For example, where multiple mineral-water reactions can be quantified, the rate of reaction of one phase may be quantified and other reactions scaled to that phase, allowing constraint of water-rock interracial area or fluid residence time. Feldspar-water reactions may be particularly useful in analyzing problems of coupled fluid flow and chemical reaction in silicate-containing terrains because dissolution rates of albite can often be unambiguously inferred from geochemical data. However, many field-based analyses of weathering rates of feldspar have shown that dissolution of feldspar in soils, aquifers, and small watersheds is slower than dissolution in laboratory experiments. In ongoing research into the dissolution kinetics of feldspars, we are investigating how the chemistry of the mineral surface affects the dissolution rate. In addition, we have analyzed field-weathered soil grains to investigate the natural surface of weathered feldspars. We are using XPS and RNRA to analyze surface chemistry of lab-leached and naturally weathered feldspars over a range of pH values. In addition, we are looking at the surface chemistry of feldspar glass and crystal after dissolution in order to investigate the structural controls on leaching. The time evolution of the mineral surface during leaching conveys important constraints on the mechanism of feldspar dissolution.

## **Mineral-Fluid Trace Element Partitioning at High Pressure and Temperature.**

J. M. Brennan, F. J. Ryerson, and H. F. Shaw, Lawrence Livermore National Laboratory

Convergent margins are one of the principal sites of mass and chemical recycling on the planet. Reactive transport, involving the generation of aqueous fluids in the subducted oceanic crust and their interaction with the overlying mantle wedge, is an important aspect of the recycling process. Although samples of the effluent fluid, such as the products of convergent margin magmatism or fluids expelled in accretionary prisms, are readily available for analysis, constraints on the source term, i.e., the initial composition of fluid prior to transecting the overlying solid matrix, are few. Inasmuch as the modification of fluid composition is one of the primary means to assess the nature of the reactive transport process, the imposition of experimental constraints on the source fluid composition is essential. Moreover, knowledge of the composition of aqueous fluids generated at depth in convergent margins serves as key input to models of global chemical cycles. As such, the major thrust of our past and on-going work is the experimental quantification of fluids generated at convergent margins, and more specifically mineral-fluid chemical fractionation of trace elements at high pressure (P) and temperature (T).

We have developed an experimental protocol for measuring mineral-fluid partition coefficients in which a known fluid composition is imposed upon a small mass fraction of mineral grains, resulting in a near-infinite reservoir of trace elements during mineral growth. Most experiments are performed using thick-walled nickel capsules lined with platinum whereby a platinum gasket and nickel lid seal the capsule during compression in the piston-cylinder apparatus. Experiments contain H<sub>2</sub>O or H<sub>2</sub>O-NaCl mixtures and added silicate material, which serves as a reasonable proxy for the major element composition of aqueous fluids that would coexist with mafic or ultramafic lithologies at high P and T. The trace element composition of minerals grown in experiments are characterized by SIMS, and run-product fluids are characterized by either mass balance or by direct analysis using isotope dilution mass spectrometry (IDMS). Experiments have been conducted at 800-1000°C and 1-2 GPa for durations of 3-4 days. To date, we have characterized mineral-fluid partition coefficients for diopsidic clinopyroxene, pyrope-almandine garnet, pargasitic amphibole and ruffe, and have preliminary results for apatite and zoisite. Elements that have been studied include Rb, Ba, Sr, Nb, U, Th, Pb, and the REEs.

Measured clinopyroxene-fluid partition coefficients for di- and trivalent cations are in excellent agreement with the Blundy/Wood partitioning model based on substitution-induced lattice strain. This result indicates that (1) trace element fractionation can be considered to be (to a first order) the result of mineral-site specificity (based solely on ionic radius and charge) and not fluid-phase complexing, and (2) partition coefficients can be extrapolated to other P and T with knowledge of the partitioning behavior of the major substituent cation, Ca. Moreover, the successful application of the Blundy/Wood model to clinopyroxene suggests that other mineral/fluid systems may be treated in a similar fashion.

Mineral-fluid partition coefficients can be used to calculate bulk eclogite- and lherzolite-fluid partition coefficients as a means to assess both the trace element composition of fluids that may be a product of dehydration of the oceanic crust and the effect of the subarc mantle on trace element fractionation during fluid flow. Results of this assessment have allowed us to provide fresh insight into certain longstanding problems related to the geochemistry of convergent margin magmas, such as their relative depletion in Nb, high Ce/Pb ratios, excesses in [<sup>238</sup>U] relative to [<sup>230</sup>Th] and the effects of fluid vs. melt metasomatism. In addition, our results afford the opportunity to evaluate the composition of material returned to the deep mantle during subduction, which in turn provides constraints on geodynamic models concerning the fate of subducted oceanic crust.



Ongoing work in our laboratory involves characterizing the chemical and isotopic partitioning behavior of light elements such as B, Be, and Li, which appear to be conservative tracers of oceanic crust dehydration. In addition, we are applying the Blundy/Wood partitioning model to accessory minerals with the goal of assessing their retentivity for REEs and actinides (e.g., Pu) during hydrothermal processes.

## A New Method for Determining Excess Gibbs Energies in Binary Metal-Carbonate Solid Solutions.

W. H. Casey and P. A. Rock, Department of Land, Air and Water Resources and the Department of Geology and the Department of Chemistry, University of California at Davis

Objective: Our objectives are (1) to establish the electrochemical cell methods involving cells without liquid-liquid junctions for determining the Gibbs energies of impure carbonate minerals, binary carbonate solid solutions, and hydroxy-carbonate minerals and oxalates of environmental interest; and (2) use of the data obtained together with literature data to test theoretical models of lattice energies and excess Gibbs energies of mixing for metal carbonate solid solutions.

Project Description and Results: Electrochemical and thermochemical measurements have been used to determine the Gibbs energies of formation and excess Gibbs energies of mixing at 25 °C and 1 bar for the systems<sup>1,2,4</sup>  $\text{Ca}_x\text{M}_{1-x}\text{CO}_3(\text{ss})$  ( $\text{M}^{2+} = \text{Cd}^{2+}, \text{Sr}^{2+}$  and  $\text{Mn}^{2+}$ ,  $0 \leq x \leq 1$ ) and excess enthalpies of formation for the system  $\text{Ca}_x\text{Sr}_{1-x}\text{CO}_3(\text{ss})$  have been measured.<sup>5</sup> We have also investigated huntite<sup>3</sup> and dolomite and obtained preliminary results on high magnesian calcites. New cells without liquid-liquid junction have been used to determine the Gibbs energies of formation of hydrocerrusite and hydrozincite.

Theoretical lattice energies and excess Gibbs energies of formation have been calculated for the systems  $\text{Ca}_x\text{M}_{1-x}\text{CO}_3(\text{SS})$  ( $\text{M}^{2+} = \text{Cd}^{2+}, \text{Mn}^{2+}, \text{Fe}^{2+}, \text{Mg}^{2+}$ ). The calculations separately evaluate the electrostatic energy polarization energy, and repulsion energy, of the crystals. As is known, the largest contribution to the lattice energy is electrostatic, followed by the repulsive energy contributions, which typically account for about 10% of the total lattice energy. The contribution from the polarization energy is of the order of 2% of the entire lattice energy, but comparable in magnitude to  $G^E$  values for metal carbonate solid solutions. The basic approach being employed by our student, Mr. Greg Mandell, for finding the polarization energies involves computing the local electric field at a reference oxygen atom due to the lattice of point charges and oxygen dipoles. The polarizability of oxygen in the solid is computed through the general Lorent local-field method of Lawless and DeVries. The partial charge on the oxygens is calculated via molecular orbital methods.

### Publications:

1. P.A. Rock, W. H. Case, M. K. McBeath, E. M. Walling. A new method for determining Gibbs energies of formation of metal-carbonate solid solutions 1: The  $\text{Ca}_x\text{Cd}_{1-x}\text{CO}_3(\text{s})$  system at 298 K and 1 bar. *Geochim. Cosmochim. Acta* (1994) **58**, 4281-4291.
2. W.H. Casey, P. A. Rock, M. K. McBeath, E. M. Walling, J-B. Chung. A new method for determining excess Gibbs energies in binary metal-carbonate solid solutions. 1994 Goldschmidt Conference; *MineralMag.* (1994) **58A**, 156-157.
3. E.M. Walling, P. A. Rock, W. H. Casey. The Gibbs energy of formation of huntite,  $\text{CaMg}_3(\text{CO}_3)_4$  at 198 K and 1 bar from electrochemical cell measurements. *Amer. Min.* (1995) **80**, 355-359.
4. W.H. Casey, P. A. Rock, J-B. Chung, E. M. Walling, M. K. McBeath. Gibbs energies of formation of metal-carbonate solutions 2: The  $\text{Ca}_x\text{Sr}_{1-x}\text{CO}_3(\text{s})$  system at 298 K and 1 bar. *Amer. J. Science* (1995) **296** (in press, 23 pages).
5. W.H. Casey, L. Chai, A. Navrotsky, P. A. Rock. Thermochemistry of mixing strontianite [ $\text{SrCO}_3(\text{s})$ ] and aragonite [ $\text{CaCO}_3(\text{s})$ ] to form  $\text{Ca}_x\text{Sr}_{1-x}\text{CO}_3(\text{s})$  solid solutions. *Geochim. Cosmochim. Acta* (1995) (in press).
6. U. Kubacky-Beard, W. H. Casey, J. H. Castles, P. A. Rock (in review). Standard Gibbs energies of formation of  $\text{ZnC}_2\text{O}_4 \cdot 2\text{H}_2\text{O}(\text{s})$ ,  $\text{CdC}_2\text{O}_4 \cdot 3\text{H}_2\text{O}(\text{s})$ ,  $\text{Hg}_2\text{C}_2\text{O}_4(\text{s})$  and  $\text{PbC}_2\text{O}_4(\text{s})$  at 298 K and 1 bar. *Geochim. Cosmochim. Acta* (1996) (submitted 12/22/95).

### **Stable Isotope Exchange Equilibria and Kinetics.**

D. R. Cole, J. Horita, S. M. Fortier, D. J. Wesolowski, L. R. Riciputi, B. A. Paterson, and T. E. Burch, Oak Ridge National Laboratory; J. W. Valley, University of Wisconsin at Madison; and A. C. Lasaga, Yale University

Equilibrium isotope fractionation factors and rates of isotope exchange (via diffusion or mineral transformation mechanisms) form the cornerstones for interpretation of stable isotope data from natural systems. Because of recent advances in analytical techniques (high precision on small sample sizes or *in situ* spots), the need for accurate, reliable fractionation factors and rate constants has never been greater. A major focus of our BES research is the experimental determination of rates and equilibrium fractionations for a variety of geologically relevant systems including, but not limited to, C-O-H gases, iron oxides, carbonates, quartz, and sheet silicates).

Experimental studies were conducted to examine the kinetics of isotope exchange and equilibrium isotope partitioning between CO<sub>2</sub> and CH<sub>4</sub> at elevated temperatures. Experiments employing CH<sub>4</sub> with 99% <sup>13</sup>C and normal CO<sub>2</sub> (-1.1% <sup>13</sup>C) showed that, in the absence of catalytic materials, the carbon isotope exchange is extremely sluggish (<0.01% exchange) even at 400°C after 26 days. Silica gel, molecular sieve, and graphite all slightly increased the isotope exchange rate. As an alternative, we tested several silica-supported metal catalysts (Ni, Pd, Pt, Rh). A detailed series of carbon isotope exchange experiments were carried out using an Ni catalyst, Ni/NiO, as an fO<sub>2</sub> buffer and two isotopically different CO<sub>2</sub> gases (50 and -40‰) that bracket the CH<sub>4</sub>. Isotopic reversal experiments demonstrated that C isotope equilibrium between CO<sub>2</sub> and CH<sub>4</sub> was reached, or very closely approached, at temperatures from 200 to 500°C after 1-4 weeks. The measured fractionation factors agree well with the calculations by Richet et al. (1977) at 200-250°C, but deviate with increasing temperature.

Oxygen isotope fractionations between magnetite-water and hematite-water have been studied over temperature ranges of 300-600°C and 150-350°C, respectively. The hematite experiments involved the simple recrystallization of fine-grained starting hematite (0.2-2.0 gm) reacted with four isotopically labeled waters. The degree of exchange ranged from <10% at 150°C to over 60% at 350°C for reaction times of 2000-2100 hrs. The fractionation factors are -10 ± 1, -8.3 ± 0.3, and -5.9 ± 0.5‰ at 150, 300, and 350°C, respectively. A number of reaction paths were used to study magnetite-water fractionation: hematite reduced to magnetite in pure water or dilute NaCl, hematite reacted with dilute acetic acid, iron metal oxidized to magnetite, and magnetite recrystallized to magnetite. CO<sub>2</sub> laser extraction (bulk) and ion microprobe (coarse single crystals) were used to analyze run products. Fractionation factors for 450°C and above agree well with those cited in the literature; between 450 and 300°C, we observe an apparent minimum of about -8.5‰ in 1000 ln α. A similar minimum was reported in theoretical studies by Becker and Clayton (1976) and Zheng (1991), but at somewhat lower temperatures, -200°C and 300°C, respectively.

Rates of isotopic exchange between minerals and fluids have been measured for a variety of mineral systems at elevated temperatures and pressures. The ion microprobe was used to measure the oxygen and carbon diffusion coefficients for the system calcite-H<sub>2</sub>O-CO<sub>2</sub> from 500 to 700°C at pressures of 0.75 to 2.75 kbar. Oxygen and hydrogen diffusivities have been determined for the systems brucite-H<sub>2</sub>O and clinocllore-H<sub>2</sub>O at 500°C and 1.5 kbar. In systems where recrystallization is the dominant mechanism, rates of isotope exchange have been measured from 300 to 500°C in the systems carbonates (Ca, Mg, Ba, Sr) - H<sub>2</sub>O, and phyllosilicates (muscovite, biotite, chlorite) - H<sub>2</sub>O, and range from 10<sup>-10</sup> to 10<sup>-7</sup> moles O /m<sup>2</sup>/s<sup>-1</sup>.

Within any given mineral group at a constant temperature, we observe a good correlation between increasing rate and a decrease in the electrostatic lattice energy.

## **Radiogenic Isotope Studies of Reactive Transport in Groundwater.**

D. J. DePaolo, M.E. Conrad, T. M. Johnson, and D. P. Schrag, Berkeley Center for Isotope Geochemistry, Department of Geology and Geophysics, Lawrence Berkeley National Laboratory, and University of California at Berkeley

Transport of solutes in groundwater must be quantified in order to predict the dispersal of contaminants in the subsurface. Even in low-temperature systems there is chemical reaction between fluid and rock accompanying the flow, and the rate of reaction affects the transport of the solutes. Although kinetic data have been determined on many relevant reactions, the actual rates of fluid-rock exchange are dependent on the effective surface area of reaction which is typically not known well enough to be a useful predictor. Isotope ratios in fluids are in many cases sensitive to the rate of fluid-rock reaction ( $R$ ), modified by the fluid velocity ( $V$ ). Our approach to the problem has been to attempt to understand how field-scale observations of isotopic ratios in fluids and rocks can be used to determine  $V/R$ , which is an effective "reaction length" ( $L$ ). Rather than try to predict  $R$ , which may be impossible, we simply try to "image"  $L$ . Regions of large  $L$  correspond to either enhanced hydraulic conductivity or suppressed reaction, and vice versa. The ambiguity of interpreting  $L$  values in terms of  $V$  or  $R$  can usually be addressed by considering other data or age constraints. Characterizing geologic fluid-rock systems at the field scale removes the uncertainty inherent in predicting the field-scale behavior from observations made at small scales (like permeabilities), and in many situations helps to answer the important regulatory questions more directly.

Our approach to this problem began with ironing out the theory for one-dimensional systems, and then doing studies of systems that can be adequately characterized. Deep sea oozes represent excellent one-dimensional systems, and we have used the approach to understand rates of diagenetic reactions and how the solid matrix is changed over time by continued reaction with the pore fluids. The latter has allowed us to strip the effects of diagenesis from paleotemperature measurements and determine paleotemperatures back into the Cretaceous, as well as estimate the oxygen isotopic composition of the glacial oceans. The models have also been applied to vadose zone transport near Yucca Mountain, where we show that the vein carbonate data (collected by USGS) indicate faster downward transport than is predicted by standard percolation models. In another study, we applied the approach to the groundwater beneath LBNL and were able to estimate the flow velocities and hence the time required to transport any contaminants offsite. In an ongoing study of fluids from the Hawaii Scientific Drilling Project core-hole in Hilo, we have enough Sr isotope measurements and other constraints to estimate the water-rock reaction rate for seawater circulating through the volcanic pile. There are now plans to meld this approach systematically with hydraulic properties measurements at a field site.

The groundwater modeling approach has also been exported to metamorphic and igneous petrology applications. Fluid-rock reaction under metamorphic conditions can be treated much like groundwater problems, our contribution being that we set up the problem without requiring rock-fluid equilibrium, but rather leaving the reaction rate as an adjustable parameter and examining the effect of varying the Damkohler number. We have used isotopic data to extract effective reaction rates and ionic diffusivities from metamorphic rocks. Similarly, isotopic data from Hawaiian lavas have been used to estimate the effective dispersivity of the partially molten zone under Hawaii, which appears to match that observed in groundwater systems at the 10 to 100km scale.

## **Origin and Timing of Fluid Flow Events in a Fault Zone, Southwest England; Paleomagnetic and Geochemical Results.**

R. D. Elmore and M. Engel, School of Geology and Geophysics, University of Oklahoma

Paleomagnetic and geochemical samples were collected from organic-rich Jurassic limestones (Blue Lias) in a fault zone along the southern margin of the Bristol Channel Basin at Kilve, West Somerset, England. The Bristol Channel Basin is one of several fault-bounded sedimentary basins in the Celtic Sea/Irish Sea region in which the timing of deformation, maturation of organic matter, and hydrocarbon migration is uncertain. Deformation at Kilve consists of numerous normal faults and associated folds. Fluid flow within the fault zone is indicated by widespread calcite veining associated with the faults. The veins contain hydrocarbons.

After removal of a modern viscous magnetization at low demagnetization temperatures, a northerly and down component, which resides in magnetite, is removed from samples of the veins and the limestones. This magnetization is interpreted as a chemical remanent magnetization (CRM) that was acquired when the vein calcite precipitated. The pole position suggests remanence acquisition in the late Cretaceous-early Tertiary. Fold tests on several of the folds associated with the faults suggest that the magnetization in the limestones is synfolding. This magnetization is also interpreted as a CRM and may have been acquired during fluid alteration of the limestones.

Whilst the host limestones and calcite veins have distinct stable carbon and oxygen isotope compositions, both have radiogenic  $^{87}\text{Sr}/^{86}\text{Sr}$  values. Based on organic geochemical studies, it is tentatively suggested that a deeper, more mature unit of the Blue Lias oil shale is the source of the calcite vein bitumen. The geochemical evidence suggests that radiogenic basinal fluids precipitated the veins and altered the limestones.

## **Insights into Fault-Fluid Interactions Using Whole-rock Geochemistry.**

J. P. Evans, Department of Geology, Utah State University

We use optical and scanning electron microscopy and whole-rock geochemical analyses to investigate variations in deformation mechanisms and fluid-rock interactions in fault-related rocks from three sites along the San Gabriel fault, southern California: Pacoima Canyon, Bear Creek, and North Fork, and at two sites in Wyoming: the White Rock thrust and the East Fork thrust. At Bear Creek, North Branch of the San Gabriel fault, unaltered and undeformed granite, granodiorite, and diorite protolith bound a fault core several m thick that consists of foliated cataclasite on either side of two 20-cm thick ultracataclasite layers. A foliated cataclasite contains clays and zeolite veins which developed by alteration of protolith during slip. The ultracataclasite consists of 20-100 gm diameter feldspar and quartz fragments embedded in a clay-zeolite matrix. The matrix consists of grains <10 gm and is enriched in Fe, Mg, Mn, and Ti relative to the average composition of the protolith. In contrast, ultracataclasite at Pacoima Canyon contains little clay and zeolite and apparently evolved with little fluid-rock interaction. Whole-rock geochemical analyses of the fault rock compositions at both sites are best explained as a result of mechanical mixing with local redistribution of some elements in a closed system relative to fluids. At both sites, the ultracataclasite compositions can be modeled as the result of mixing of the bounding foliated cataclasites. Similarly, the foliated cataclasites were derived by mixing the protoliths on the same side of the ultracataclasite layer. Whole-rock analyses for rocks from the North Fork site, which lies on a major splay of the San Gabriel fault, suggest an open system relative to fluids. The concentration of immobile elements in the fault core relative to all protoliths is best explained by fluid-assisted volume loss of  $37\% \pm 10\%$ . Overall, the results imply local- and regional-scale variations in the hydrologic setting along the San Gabriel fault that produced contrasting styles of deformation and fluid-rock interactions.

The East Fork and White Rock thrusts formed at 4-7 km and 10-12 km depths, respectively, in crystalline thrust sheets in northwestern Wyoming. The fault zones consist of undeformed and unaltered protolith, which bounds damaged zones with increased fracture, fault, and vein density and chemical alteration, and a fault core comprised of zones of gouge, cataclasite, and ultracataclasite. Whole-rock geochemical analyses of major, minor, and trace elements in 26 samples document the fluid-rock interactions in the fault zones. Fault-related rocks from the shallow East Fork fault exhibit 10-40% depletion of Si, Al, K, Na, and Ca as measured against immobile Ti as reference in the damaged zone, 40-60% depletion of Ca and Na, and 0-20% depletion of Si, Al, and K in the fault core. Rocks from the deeper level White Rock thrust exhibit 10-30% depletion of these elements in protocataclasites at the edge of the fault core and up to 65% depletion in the cataclasites and ultracataclasites of the fault core. We interpret these results to show that soluble elements were removed from the fault zones by syntectonic fluid flow. Estimated volume losses in the shallow fault range from 0-22%, whereas the deeper level fault experienced 50-65% volume loss in the fault core. Silica loss is used to estimate fluid-rock ratios in the fault zones by assuming a range of temperatures and silica solubilities in the faults during deformation. Volumetric F/R ratios range from  $10^2$ - $10^4$  for both faults, which yield fluid fluxes in the fault zones of  $10^{-6}$ - $10^{-9}$  m/sec using geologic constraints on the life and geometry of the fault. Depletion and volume loss at deep levels were greater due to hotter fluids and finer grain size generated by mixed brittle plastic deformation, whereas at shallow levels, cooler temperatures and purely brittle deformation resulted in vein formation and less chemical fluid-rock interactions.

## **Two-Phase Flow in Fractures.**

R. J. Glass, Geohydrology Department, Sandia National Laboratory

In single-phase flow, geometry of the fracture aperture network determines flow and transport characteristics within single fractures. Under two-phase, immiscible fluid-flow conditions, phase-geometry (i.e., the geometry that is saturated with each phase) within the fracture ultimately controls the permeability to each phase, fluid pressure/saturation relations, and solute dispersion within each phase. Phase geometry is a function of both the aperture field and the two-phase flow processes themselves. Capillary, gravitational, and viscous forces in combination with boundary and initial conditions have all been demonstrated to play roles in the formation of fracture phase-geometry. Phase "fingering," a separate process from the single-phase concept of flow channelization, occurs in fractures where any of the aforementioned forces are dominant (capillary fingering, gravity fingering, viscous fingering).

The presentation will focus on low capillary number phase invasion processes where capillary and gravity fingers dominate. Experimental results for both imposed flux and dissolution phase invasion processes are used to develop an aperture scale model that is a modified form of invasion percolation. The effects of gravity, local aperture field geometry, and local in-plane interfacial curvature between phases are included in the calculation of local aperture phase invasion potential. This potential controls the choice of which aperture is invaded as the displacement process progresses and thus the growth of the phase saturation structure within the fracture. The modified percolation model is implemented numerically incorporating several first order approximations and used to simulate phase saturation structure growth. These calculations are compared to physical experiments in an initial air filled, analog rough-walled fracture where the angle of the fracture in the gravity field was varied. Comparison of numerical and physical experiments shows encouraging agreement. The inclusion of gravity yields fingers oriented in the direction of the gravitational gradient when the more dense fluid invades the fracture from the top. These fingers widen and tend to meander more as the gravitational gradient decreases. In-plane interfacial curvature between phases also greatly affects the phase saturation structure in both horizontal and nonhorizontal fractures, causing the suppression of capillary fingers at small scale and the formation of macroscopic fingers and fronts.



## Using MC-ICPMS to Study Mass Transfer in Low Temperature Fluid Systems.

A N. Halliday, Department of Geological Sciences, University of Michigan

Our understanding of mass transfer by low temperature fluids is limited, in part, by (1) inadequate isotopic tracers, the chemical behavior of which is well understood, (2) limited spatial resolution for isotopic tracers that could be used to study the effects of exchange and recrystallization at the sub-microscopic scale, and (3) a poorly constrained knowledge of the timing of crustal fluid flow relative to basinal evolution. Isotopic approaches using the new method of inductively coupled plasma magnetic sector multiple collector mass spectrometry (MC-ICPMS) offer considerable potential for advances in all of these areas. MC-ICPMS combines the ionization efficiency of ICP sources with the precision attainable with multiple-collector, double-focusing, magnetic-sector mass spectrometry. The addition of a laser facilitates studies for which spatial resolution is needed. Although this research is in its infancy, we can already report significant developments in each of the above areas as illustrated by the following examples.

Ocean chemistry of hafnium: The marine geochemistry of hafnium holds considerable potential for tracing hydrothermal components in the oceans and changes in fluxes through time.  $^{176}\text{Hf}$  is produced by  $\beta$  decay of  $^{176}\text{Lu}$  ( $\lambda = 1.94 \times 10^{-11} \text{ y}^{-1}$ ). The mantle has become depleted in Hf relative to Lu, the Lu/Hf ratio of the continental crust being relatively low. Therefore, the Hf in the mantle is more radiogenic and the Hf in the continental crust is less radiogenic than that of the bulk earth (which should be close to chondritic). While the Nd budget of the oceans is largely dominated by continental runoff, early results indicated that the Hf in the oceans might be more strongly dominated by hydrothermal contributions. A new extensive data set of Hf isotopic compositions from the surfaces of Mn crusts reveals greater complexity with considerable heterogeneity in  $\epsilon_{\text{Hf}}$  (-3 to +11) that is a function of crust type (hydrogenous versus hydrothermal) and location. Hydrothermal crusts have the least Hf but the highest  $\epsilon_{\text{Hf}}$ . Hydrogenous crusts have up to 10 ppm Hf and  $\epsilon_{\text{Hf}}$  values that are distinct for each ocean (Atlantic < Indian < Pacific). Hf isotopic compositions are correlated with Pb isotopic compositions, implying related removal mechanisms. Further work is in progress on eolian inputs and direct analyses of natural fluids.

Sr isotopic measurements *in situ*: We have recently demonstrated that *in situ* laser ablation sampling and analysis with MC-ICPMS is capable of accurate and precise measurement of Sr isotopic compositions in geologic materials. Sample preparation is very simple. Correcting for Rb interference is straightforward for low Rb/Sr minerals such as plagioclase feldspars, basaltic groundmass or glass, clinopyroxene and natural phosphates, sulfates, and carbonates. Correcting for Kr is more complicated because the mass bias and focusing for ions contributed from the plasma support gas are different from those of the ablated particles or solute. The resultant data for carbonates and feldspars agree with their independently known values exactly, and matrix effects appear to be negligible.

In-Sn geochronology: The dating of the products of ancient crustal fluid flow has proved extremely difficult. It is particularly important to find new ways of directly dating hydrothermal minerals such as sulfides. It would clearly be advantageous to have a method that is insensitive to uncertainty in initial isotopic composition and for which there is question that the parent/daughter ratios are being fractionated by sulfide deposition. Despite the success of Rb-Sr dating of sulfides, these problems represent a constant source of concern. For these reasons, we have been developing In-Sn geochronology,  $^{115}\text{In}$  (95.67%) decays to  $^{115}\text{Sn}$  (0.34%) with a half-life of  $4.4 \times 10^{14}$  years. The In/Sn ratio of all normal silicate and carbonate rocks in the crust and mantle is sufficiently low that the isotopic composition of Sn will not change significantly over the entire age of the earth. However, some sphalerites contain up to 2 wt % In. Therefore, In/Sn geochronology is a potentially powerful way of determining the ages of low temperature

mineralization because there is no variability in initial ratio and the In/Sn ratio is only fractionated by sulfide deposition. Therefore, any high In/Sn phase can be dated accurately on its own, with a "model" age that is calculated with a high degree of certainty regarding the initial Sn isotopic composition. Isochrons are thus effectively unnecessary. However, there are severe difficulties to be overcome. Not least of these is that nobody has previously been able to measure Sn isotopic compositions with sufficient precision to determine the small differences in  $^{113}\text{Sn}$  abundance produced by decay of the very long-lived  $^{115}\text{In}$ . Recently we have improved the precision of measurement of Sn isotopic compositions by approximately an order of magnitude. The In/Sn ratios in some sulfides (sphalerite, chalcopyrite, tetrahedrite) are found to be sufficiently high (commonly  $>5$ ) that the predicted  $^{113}\text{Sn}$  excess caused by decay of  $^{115}\text{In}$  is measurable. The In/Sn ratios determined so far range up to about 45, and preliminary In-Sn ages for Precambrian ore deposits appear to be close to their independently known age.

## U-Pb Dating of Paleocaliche.

G. N Hanson, W. J. Meyers, E. T. Rasbury, and Z. Wang, Department of Earth and Space Sciences, State University of New York at Stony Brook

The goal of this project is to develop field, petrographic, and geochemical criteria to allow high precision U-Pb dating of calcretes or caliches at paleo-exposure surfaces on carbonate and clastic rocks in rapidly deposited sediments. We have chosen to use U-Pb dating of caliche developed in paleosols because

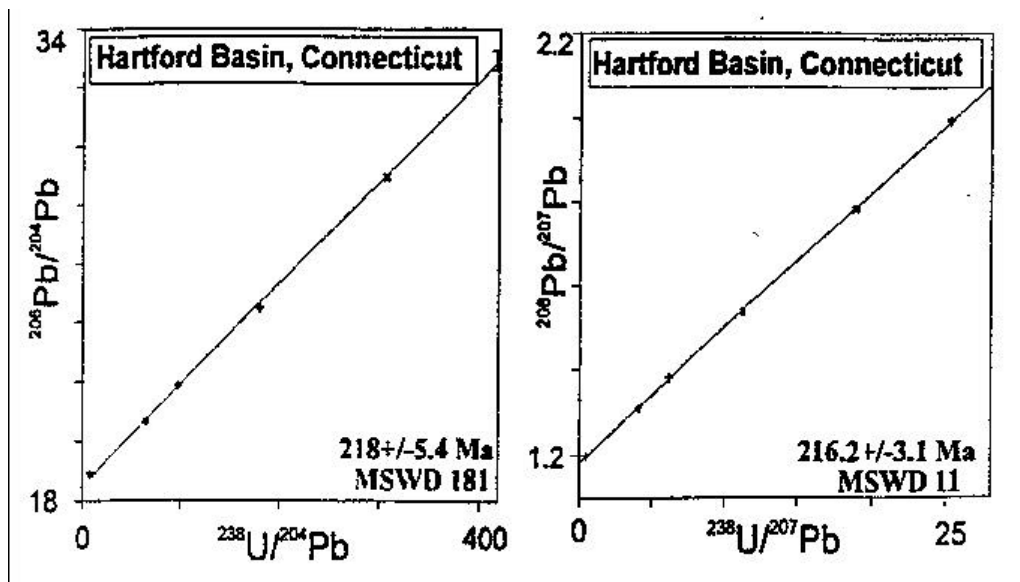
- Uranium is enriched in alkaline soil profiles.
- Caliches are common in rapidly deposited sediments throughout the Phanerozoic.
- Caliches consist of low magnesium calcite. This stable form of calcite does not easily recrystallize during later diagenesis.
- Pedogenic features can be identified geochemically and petrographically.
- U and Pb are quite different chemical, allowing significant enrichment in U relative to Pb. Yet, neither is easily mobilized during diagenesis.

We have begun studies in the Pennsylvanian-Permian section in the Sacramento Mountains, New Mexico, and in the Triassic-Jurassic section in the Hartford Basin in Connecticut. Both sections have well characterized paleosols that developed in rapidly deposited sediments. In addition, we are participating in the study of a core jointly owned by UNOCAL and the Japanese National Oil Company (JNOC). This core on the eastern edge of the Central Basin Platform of the Midland Basin, Texas, includes the interval in the Sacramento Mountains.

We describe here some of the early results on the U-Pb isochron studies on caliches from the New Haven Arkose in the Hartford Basin. Petrographic study of calcretes in the New Haven Arkose has revealed at least three generations of calcite that closely coexist in the calcretes. The first two generations are micritic and blocky calcite, respectively, which both have dull to dark cathodoluminescence. They are closely associated with root related fabrics and have negative  $\delta^{13}\text{C}$  and  $\delta^{18}\text{O}$  values and low Mn abundances typical of soil carbonate. These data are consistent with the first two generations of calcite having been precipitated during pedogenesis. The third generation is blocky calcite with bright cathodoluminescence, which fills pore spaces left by the first generation calcite. The third generation calcite precipitated after internal sediments. This calcite has a larger range of  $\delta^{13}\text{C}$  and  $\delta^{18}\text{O}$  and high Mn concentrations. While the third generation calcite may be pedogenic, it may be burial calcite or groundwater calcite. Fission track studies reveal that the first and second generations of calcite have substantially higher U abundances than the third generation.

Due to the small sample sizes that we must use, it is difficult to precisely measure the  $^{206}\text{Pb}/^{204}\text{Pb}$  ratio. It is significantly easier to measure the  $^{206}\text{Pb}/^{207}\text{Pb}$  ratio precisely. The Figure below shows two isochrons for the same data set using both  $^{238}\text{U}/^{204}\text{Pb}$ - $^{206}\text{Pb}/^{204}\text{Pb}$  and  $^{238}\text{U}/^{207}\text{Pb}$ - $^{206}\text{Pb}/^{207}\text{Pb}$  isochrons. While the ages for the two isochrons, 218 and 216 Ma, are the same within uncertainty, the  $^{238}\text{U}/^{207}\text{Pb}$ - $^{206}\text{Pb}/^{207}\text{Pb}$  isochron has an uncertainty about one-half that of the  $^{238}\text{U}/^{204}\text{Pb}$ - $^{206}\text{Pb}/^{204}\text{Pb}$  isochron. The Triassic-Jurassic boundary occurs at the top of the 1500 to 2500 meter thick New Haven Arkose. The age of the boundary is  $208 \pm 16$  Ma [2 signal] (Harland et al, 1990). The calcrete selected for dating is 100 to 200 meters below the top of the New Haven Arkose based on the stratigraphy of Dowdall, 1979. The Talcott basalt which immediately overlies the New Haven Arkose has an Ar-Ar age of  $187 \pm 3$  Ma, which may be a minimum age for intrusion (Seidemann, 1989). The  $216 \pm 3$  Ma age of the calcrete is consistent with the geology and other ages. It will be necessary to now date calcretes above the Jurassic-

Triassic boundary to put constraints on the age of the boundary, as well as to date calcretes deeper in the section to see if variations in the ages are consistent with the stratigraphic relations.



## **K-feldspar Thermochronometry.**

T. M. Harrison, Department of Earth and Space Sciences, University of California at Los Angeles

Because most geophysical processes involve heat flow disturbances, recovery of temperature histories can provide insights into the behavior of the lithosphere that might otherwise be inaccessible. The  $^{40}\text{Ar}/^{39}\text{Ar}$  method has the potential to furnish information about both the internal distribution of  $^{40}\text{Ar}^*$  and Ar diffusion parameters of minerals. Our multi-diffusion domain model (MDD) has shown promise in reconciling once problematic effects seen in step-heating results of K-feldspar and is now ready for application to a number of energy related problems. In our formulation of the MDD model, the form of the Arrhenius plot and age spectrum are a function of the diffusion parameters for each discrete domain (activation energy,  $E$ , and frequency factor,  $D_0$ ), the domain distribution parameters (domain size,  $\rho$ , and volume fraction,  $\phi$ ), and the thermal history. Since the diffusion parameters may be obtained directly from the Arrhenius plot and we have two independent measures of  $\rho$  and  $\phi$  (the Arrhenius plot and age spectrum), we have sufficient information to obtain a solution for the thermal history for the case of monotonic cooling. The three studies described below represent the completion of long-term investigations of the underlying assumptions and general predictions of the theory.

An early proposal to explain the relatively low argon retentivity in K-feldspars invoked perthite lamellar boundaries as paths of fast diffusion, effectively reducing the length scale for argon diffusion and lowering the closure temperature. This idea was criticized as these interfaces were usually coherent and thus thought not able to behave as zones of rapid diffusion. To address this issue, we utilized Ne isotopes as a probe of the diffusion behavior in and around perthite lamellae during laboratory step-heating. During the neutron irradiations to affect the  $^{39}\text{K}(n,p)^{39}\text{Ar}$  reaction, reactions on Na produce all three Ne isotopes. The nature of Ne loss from the sample can thus lead to insights into the role of perthite boundaries in facilitating diffusive transport and/or as a monitor of the lamellar annealing. We have found that, unlike feldspar glasses, Ne diffusivities of crystalline material exhibit nonlinear Arrhenius arrays topologically identical to those obtained for Ar diffusion in K-rich alkali feldspar, which we attribute to the existence of discrete domains of Ar retentivity. The Bishop Tuff sanidine, which has a well defined lamellar spacing of  $155 \pm 6$  nm and high Na content, is characterized by enhanced Ne loss at low temperatures requiring that exsolution boundaries to be permeable to rare gas transport.

A comprehensive survey of the Ar diffusion properties of  $>100$  K-feldspars analyzed in  $^{40}\text{Ar}/^{39}\text{Ar}$  step-heating experiments has permitted us to test address fundamental issues underlying the multi-domain hypothesis. We developed statistical methods based upon the correlation theorem to determine the extent to which the age and  $\log(r/r_0)$  plots exhibit the sympathetic behavior predicted by the MDD model. Correlated behavior is expected only if Ar diffusion occurs by the same mechanisms and uses the same diffusion boundaries in nature as it does in the laboratory heating. The model predicts that the age spectrum and  $\log(r/r_0)$  plots will be highly correlated when all domains experience uniform fast or slow cooling. Experimental data from samples satisfying these criteria show this high correlation. Correlation is significantly reduced if age and Arrhenius results from different samples are mixed. Samples highly contaminated with excess  $^{40}\text{Ar}(^{40}\text{Ar}_E)$  have poorly correlated age and Arrhenius data. However, the relationship (MR CLEAN) between the differential release of  $^{40}\text{Ar}_E$  and  $C1/K$  between successive temperature pairs during laboratory heating permits us to correct age spectra for Cl-correlated  $^{40}\text{Ar}_E$ , which dramatically increases the correlation to values predicted by synthetic results.

We have developed an approach for automating K-feldspar thermal history modeling that greatly reduces operator bias. Codes for both monotonic cooling and general thermal histories allowing reheating (based upon use of Chebyshev polynomials) produce best-fit solutions from

generalized initial temperature-time histories. Through a variational process, an optimum fit to the laboratory age spectrum is obtained. Under the constraint of monotonic cooling, the thermal history solution is unique. When this constraint is relaxed, however, a variety of solutions that fit the age spectrum are obtained. Contour plots of the probability density calculated from this spectrum of solutions reveal the full range of T-t constraints afforded by the K-feldspar age and kinetic results. Because the approach is a variational process that calculates best-fit cooling histories using the age spectra, it is a significant improvement over Monte Carlo routines that calculate age spectra from random T-t histories.

Early attempts to evaluate the thermal history of sedimentary basins from  $^{40}\text{Ar}/^{39}\text{Ar}$  measurements of detrital K-feldspars were hampered by their treatment as single diffusion domain and the ubiquitous presence of  $^{40}\text{Ar}_\text{E}$ . Armed with the MDD model and MR CLEAN, we have returned to the San Joaquin Basin and analyzed K-feldspars from arkosic sandstones from a depth of 4.12 and 6.61 km. These preliminary results yield burial histories that are internally consistent and match the predictions of previous backstripping models.

## **Fluid Compositional Changes in Petroleum Reservoirs Recorded by O Isotope Analyses of Quartz Overgrowths.**

R L Hervig and L B. Williams, Center for Solid State Sciences, Arizona State University

Introduction: We have obtained microanalyses of  $\delta^{18}\text{O}$  in authigenic quartz cement from oil-producing sandstones using secondary ion mass spectrometry (SIMS) following the procedure of Hervig et al. (*Int. J. Mass Spec. Ion Proc.* (1992) **120**, 45-63). These data allow us to devise models for the chemical evolution of pore fluids.

Samples: Sandstones from the Texas Gulf Coast, the Western Canadian Sedimentary Basin, and the North Sea have been studied using this technique. The latter two of these oil-producing fields show similar burial histories: a period of >100 Ma with very low rates of deposition at

temperatures <50 °C followed by a period of rapid burial over a few tens of Ma where the sandstones reached temperatures of >100 °C. The Texas samples experienced more rapid burial to ~80°C followed by uplift for ~5 Ma and subsequent burial (at rates similar to the initial burial) with temperatures increasing to ~120°C.

Results: Maximum and minimum  $\delta^{18}\text{O}$  values of authigenic silica from the Texas and Canadian sandstones are 34‰ and 20‰, respectively, and 27‰ and 13‰ for the North Sea samples. The deepest North Sea sandstones contained authigenic rims thick enough to test for zoning; quartz closest to the detrital grains were near 24‰, with subsequent precipitates decreasing to 13‰. At the edge of the quartz  $\delta^{18}\text{O}$  increased to 20‰.

Discussion: The microanalyses do not allow a unique history to be determined for any sample set because of assumptions about the nature of pore fluids (i.e., their temperature and oxygen isotopic composition). However, the simplest model that can be used to describe all the localities involves minor precipitation of quartz from meteoric waters ( $\delta^{18}\text{O}$  from -10 to -2‰) at low temperature followed by increasing precipitation at  $T > 50^\circ\text{C}$  from diagenetically altered fluids ( $\delta^{18}\text{O}$  from +2 to +10‰) during periods of more rapid burial. The abundance of quartz precipitated at  $T > \sim 120^\circ\text{C}$  appears to be very low in all cases.

There are published data on Norwegian meteoric water and well waters associated with the North Sea samples that allow us to calculate (using EQ3/6) the amounts of quartz that might precipitate during diagenesis and see if this matches our simple models as defined by the zoning of quartz precipitates. These calculations suggest that the amount of quartz precipitating from meteoric water will be very low, but will increase significantly when low pH diagenetic fluids are mixed in. Continued burial in the presence of diagenetic fluids results in minor precipitation because of the increase in silica solubility at these higher temperatures. The modeling suggests that mass transport of  $\text{SiO}_2$  is not required but that acid provided by reactions in shales drives the dissolution of silicates (mica, K-feldspar, kaolinite) in the sandstone to provide all the quartz cement observed.

Conclusions: Our microanalyses reveal significant variations in diagenetic quartz chemistry that must reflect changing fluid compositions as well as changing temperature. All rocks from oil-producing reservoirs that we have studied have shown broadly similar trends. These trends indicate that most authigenic quartz precipitates when meteoric pore fluids are joined by a significant diagenetic component. Future work will involve using other chemical information from quartz (trace elements) and clays (O, B isotopes) to help unravel the diagenetic process.

## Salt Effects on Stable Isotope Partitioning.

J. Horita, D. R. Cole, D. J. Wesolowski, and S. M. Fortier, Geochemistry Group, Chemical and Analytical Sciences Division, Oak Ridge National Laboratory

Essential to the use of stable isotopes as natural tracers and geothermometers is the knowledge of equilibrium isotope partitioning between different phases and species, which is usually a function of temperature only. The one exception known to date is oxygen and hydrogen isotope fractionation between liquid water and other phases (steam, gases, minerals), which changes upon the addition of salts to water, i.e., the "isotope salt effect." To date, knowledge of this effect, the difference between activity and composition ( $\alpha$ -X) of isotopic water molecules in salt solutions, is very limited and controversial, especially at elevated temperatures. From our detailed, systematic experimental study at Oak Ridge, a simple, coherent picture of the isotope salt effect is emerging that differs markedly from the complex results reported in the literature.

The isotope effect in salt solutions ( $\mathbf{G}$ ) can be experimentally determined from the equation  $10^3 \ln \mathbf{G} = 10^3 \ln \mathbf{a}_{\text{A-salt soln}} - 10^3 \ln \mathbf{a}_{\text{A-pure water}}$ , where A represents oxygen- and/or hydrogen-bearing substances in isotopic equilibrium with water, and  $\mathbf{a}$  the equilibrium fractionation factor. In our experiments, the isotope salt effect was determined in two different systems: (1) liquid-vapor water equilibration in the system Na-K-Mg-Ca-Cl-SO<sub>4</sub>-H<sub>2</sub>O from 50 to 350°C, and (2) mineral (calcite, strontianite, and brucite)-water isotope exchange from 200 to 500°C. Our results of liquid-vapor isotope fractionation of pure water and single salt solutions (NaCl, KCl, MgCl<sub>2</sub>, CaCl<sub>2</sub>, Na<sub>2</sub>SO<sub>4</sub>, and MgSO<sub>4</sub>) showed the values of  $10^3 \ln \mathbf{a}(\mathbf{D})_{\text{liquid-vapor}}$  for the salt solutions studied were always smaller (up to 20‰) than that of pure water at a given temperature (i.e., positive  $10^3 \ln \mathbf{G}(\mathbf{D})$  values). In contrast, values of  $10^3 \ln \mathbf{a}(^{18}\text{O})_{\text{liquid-vapor}}$  for the salt solutions were higher than, or very close to, that of pure water except for KCl solutions near room temperature (i.e., negative  $10^3 \ln \mathbf{G}(^{18}\text{O})$  values). The results for NaCl solutions to 350°C show that the effect of NaCl on the oxygen and hydrogen fractionation factors increases with increasing temperature above about 200°C. Measured values of  $10^3 \ln \mathbf{G}$  for complex mixed salt solutions between 50 and 100°C, some of which simulate natural geothermal brines (e.g., Salton Sea), agree well with values calculated from a simple summation of the effects of individual salts in the mixed solutions.

The following experiments have been conducted to date on mineral-water systems:

- (1) CaCl<sub>2</sub> - H<sub>2</sub>O  $\pm$  NaCl at 300°C and 1 kb,
- (2) SrCO<sub>3</sub> - H<sub>2</sub>O  $\pm$  NaCl at 300 and 450°C (P = 0.1 and 1 kb), and
- (3) Mg(OH)<sub>2</sub> - H<sub>2</sub>O  $\pm$  NaCl or MgCl<sub>2</sub> at 200-500°C (P = 21-800 b).

Our results obtained from the mineral-water experiments are very similar to those of our liquid-vapor experiments in the same temperature range. The results at 500°C indicate that the isotope salt effect keeps increasing with increasing temperature, and that its magnitude may not be linear with NaCl concentrations at elevated temperatures. The effect of MgCl<sub>2</sub> on the value of  $10^3 \ln \mathbf{a}(\mathbf{D})_{\text{brucite-water}}$  appears to be 2-3 times larger than that of NaCl, as is the case for the liquid-vapor system. Preliminary results from the system SrCO<sub>3</sub> - H<sub>2</sub>O  $\pm$  NaCl at 450°C indicate that the effect of NaCl on the value of  $10^3 \ln \mathbf{a}(\mathbf{D})_{\text{strontianite-water}}$  could be as large as -0.35‰/molal. Very consistent results obtained from the two different experimental systems strongly suggest that the isotope salt effects are a common feature of the isotope fractionation between brines and any other coexisting phases (gases, minerals, dissolved species) even at elevated temperatures.

Rather large isotope salt effects observed in our experiments even at elevated temperatures have to be taken into account in many geochemical processes involving brines such as



boiling/condensation, mineral precipitation, and hydrothermal alteration of rocks. Isotope fractionation factors in the systems liquid-vapor water and mineral-water, which are in wide use as isotope geothermometers, should be corrected accordingly for the isotope salt effect.

### **Brine Mobility in Matrices with Retrograde Solubilities.**

M. C. Johnson, Department of Geography and Environmental Engineering, United States Military Academy, and D. Walker, Lamont-Doherty Earth Observatory

Most minerals have prograde solubilities; they are more soluble in hot water than in cold water. Several sulfate species, however, have retrograde solubilities. For example, the aqueous solubility of  $\text{Li}_2\text{SO}_4 \cdot \text{H}_2\text{O}$  has been measured and decreases substantially from 3.2 molal at 20°C to 2.9 molal at 80°C. In a thermal gradient, solubility differences with temperature in the presence of crystals drive diffusive mass movement through the fluid. This process has been observed in silicates and aqueous brines. For minerals such as  $\text{Li}_2\text{SO}_4 \cdot \text{H}_2\text{O}$  with retrograde solubility, solute migrates from cold to hot. Retrograde solubility may be offset, however, if the Soret coefficient for  $\text{Li}_2\text{SO}_4 \cdot \text{H}_2\text{O}$  is large and prograde. In fact, observation of  $\text{Li}_2\text{SO}_4 \cdot \text{H}_2\text{O}$  brines suggests that the Soret effect for  $\text{Li}_2\text{SO}_4 \cdot \text{H}_2\text{O}$  in aqueous solutions over this temperature range, although prograde, is modest. This observation agrees with extrapolation from similar systems. Therefore, brine pockets in an  $\text{Li}_2\text{SO}_4 \cdot \text{H}_2\text{O}$  matrix should migrate by dissolution and reprecipitation in a thermal gradient from regions of high temperature to low temperature. We tested this prediction by placing  $\text{Li}_2\text{SO}_4 \cdot \text{H}_2\text{O}$  crystal/brine saturated solutions in clear Plexiglas tubes. These mixtures were indeed observed to expel brine to their cold ends while growing compact, brine-free  $\text{Li}_2\text{SO}_4 \cdot \text{H}_2\text{O}$  crystal piles at their hot ends. While gravity might be expected to assist in separating brine from crystals when the cold end is on the top, this behavior also occurred when the cold end was on the bottom (producing a gravitationally unstable configuration of crystals on top of brine). Prograde soluble NaCl crystal/brine solutions were also observed under the same experimental conditions. As expected, these matrices expelled brines to their hot ends. Elongated textures *parallel* to the thermal gradient were observed within the  $\text{Li}_2\text{SO}_4 \cdot \text{H}_2\text{O}$  crystal/brine solutions. This sense of elongation is also observed in the thermal migration of silicate crystals in melts in which they have prograde solubilities. These textures differ from the textures reported in the literature for prograde soluble chlorides, which tend to produce elongated textures *perpendicular* to the thermal gradient. This difference may imply that the expulsion processes in sulfates and chlorides is controlled by different factors. This migration also accords with the observed slow time scales of sulfate thermal migration. Whereas silicates respond on time scales predicted from known diffusivities, sulfates and chlorides are much slower, possibly as a consequence of dissolution and precipitation kinetics. Many details of the thermal migration process are not yet understood, although it is clear that a wide range of information is present in the petrographic detail of the matrices. The observation of retrograde solubilities is more than a scientific curiosity. The rapid thermal migration of brines away from heat sources suggests that retrograde soluble materials may make ideal backfill for nuclear waste repositories where corrosion of canisters by ground water is an ever-present worry. In this respect,  $\text{Li}_2\text{SO}_4 \cdot \text{H}_2\text{O}$  serves as a high-solubility analog material with kinetic properties useful for laboratory demonstration.  $\text{CaSO}_4 \cdot 2\text{H}_2\text{O}$  or  $\text{Na}_2\text{SO}_4 \cdot \text{H}_2\text{O}$  may be more practical choices than  $\text{Li}_2\text{SO}_4 \cdot \text{H}_2\text{O}$  for actual engineering applications.

## **The Composition of Noble Gases in Fluids Associated with the San Andreas and Companion Faults.**

B. M. Kennedy, A. Ellwood, and D. J. DePaolo, Berkeley Center for Isotope Geochemistry, Lawrence Berkeley National Laboratory

Lack of a heat flow anomaly across the San Andreas Fault (SAF) suggests fault weakness in an absolute sense: failure occurs under much smaller shear stress than inferred from laboratory friction measurements (Lachenbruch and Sass, 1980). A mechanically stronger adjoining crust suggests relative fault weakness: implied by the high angle of maximum horizontal stress with the trace of the SAF (Zoback *et al.*, 1987). Fault weakness is due either to a transient or unusually low coefficient of friction, or fault zone fluid pressures may be permanently or transiently greater than hydrostatic (e.g., Huber and Rubey, 1959).

Proposed models for SAF weakness are similar in mechanics but differ in the source of pressurized fault zone fluids. (1) Byerlee (1990, 1993): fluids are derived from the brittle upper crust. In the fault zone, fluids become trapped and high pore pressures develop from compaction of fault zone materials. (2) Sleep and Blanpied (1992): fluids are supplied by direct meteoric infiltration through a series of crack networks. The cracks are isolated and compacted during shearing. (3) Rice (1992): fluids are supplied from a region near the ductile root of the fault zone by a pressurized mantle-fed source. The fault core-country rock boundary is impermeable; thus high fault zone pore pressures are maintained.

Helium isotopic compositions ( $R/R_a$ ) in well and spring fluids associated with the San Andreas and companion faults range from 0.12 to 4.0. The fluids issue from three primary rock types: (1) Jurassic-Tertiary Great Valley Sequence sedimentary and volcanic rocks, (2) Mesozoic Salinian granitic rocks, and (3) Jurassic-Cretaceous Franciscan graywackes and metagraywackes. Typical continental crustal fluids and rocks are expected to have  $R/R_a$  of  $<0.1$  (Mamyrin and Tolstikhin, 1984). In that context, all the sampled fluids are enriched in  $^3\text{He}$ , suggesting a mantle component pervades the fault zones. Its presence supports the Rice (1992) fault weakness model. Using the fluid composition of the geopressed Varian Well ( $1.7 R_a$ ,  $1.9 \times 10^{-9}$  moles  $^4\text{He}$ -fluid), located within the creeping Parkfield segment of the SAF, and assuming a mantle source at the base of the ductile transition zone ( $8 R_a$ ), a 1-d-advective-steady state flow model yields an upward fluid flow rate through the fault zone of  $\sim 2\text{--}4$  mm/yr, consistent with the preferred Rice (1992) upflow rate.

Fault zone fluid chemistries (Thordsen *et al.*, 1995), however, indicate variable mixing of at least four fluids, depending on locality: (1) dilute meteoric water, (2) Franciscan fluids (high  $\text{B}/\text{Cl}$ ,  $\text{SO}_4$ -poor), (3) Salinian fluids (low  $\text{B}/\text{Cl}$ ,  $\text{SO}_4$ -rich), and (4) Great Valley fluids (high total salinity, low  $\text{B}/\text{Cl}$ ,  $\text{SO}_4$ -poor). Probable mixing of mantle- and crustal-derived fluids within the fault zones suggests that (1) the upflow rates calculated from helium contents and isotopic composition are upper limits, and (2) components of each of the proposed models (Rice, 1992; Byerlee, 1990 and 1993; and Sleep and Blanpied, 1992) may contribute to fault weakness.

## High-Resolution Ion Microprobe Measurements of Isotopic Tracers for Understanding Geothermal and Petroleum Reservoir Histories.

K D McKeegan, Department of Earth and Space Sciences, Lawrence Livermore National Laboratory

Advances in geochemical instrumentation that permit interrogation at new levels of sensitivity and spatial scales often lead to novel insights into earth processes. The high-resolution ion microprobe has the potential to quantitatively utilize isotopic and chemical tracers, such as accessory minerals or light stable isotopes, to reveal important information regarding thermal and volatile histories in crustal systems. We have commissioned a new generation ion microprobe, the CAMECA ims 1270, and developed two principal applications that give the nation a new capability for energy-related studies: U-Th-Pb accessory mineral dating and *in situ* measurement of carbon and oxygen isotope abundances.

We have developed the capability to perform U-Th-Pb isotopic measurements on zircon and monazite utilizing a calibration relationship that takes advantage of the contrasting energy distributions of U and Th atomic ions relative to that of their oxides and  $\text{Pb}^{+}$ . Based on measurements of numerous standards, precision and accuracy of zircon and monazite ages, varying between 20 and 3,000 Ma, are typically better than +2%. We have utilized this methodology to reveal diffusion gradients of radiogenic Pb in restitic monazites. Coupled with knowledge of monazite solubility and the diffusion behavior of Pb in monazite, we can estimate the timescale of melting and transport. For example, applied to peraluminous granitoids from the Himalayas, this approach yields estimates between 0.5 and 1.5 Ma which tightly constrain the possible segregation and ascent mechanisms. This information is directly relevant to understanding geothermal budgets and is not easily obtained otherwise.

We are currently developing techniques for measuring oxygen isotope ratios of silicates as well as oxygen and carbon isotopes in carbonates on a small spatial scale ( $<20\text{ }\mu\text{m}$ ) using polished thin sections. Ion microprobe analyses of two calcite standards yield precise ( $\pm 0.5\text{‰}$ ) results that agree within 0.3‰ of the oxygen and carbon isotopic ratios determined by conventional methods. Diagenetic carbonate cementation of sandstone reservoirs has a major impact on the mobility and recovery of liquid hydrocarbons. Carbonate cements within these reservoirs are generally precipitated from waters migrating from deeper levels during petroleum maturation. While oxygen isotopes can yield information regarding the thermal history of the basin, carbon isotopes measured in the same cements can trace the sources of carbon and thus be linked to the generation of petroleum. *In situ* measurements are required because multiple phases of cementation are generally present. These results not only constrain aspects of the volatile history, but also the evolution of the reservoir permeability. Oxygen isotope ratios measured in olivines yield 1‰ accuracy for  $\delta^{18}\text{O}$  and  $<2\text{‰}$   $\delta^{17}\text{O}$ . The initial application of this approach has determined oxygen isotopic ratios of rare olivine and pyroxene in CI chondrites, which are compositionally the most primitive solar system materials.

### **Magmatic and Aqueous Fluids: Constraints from U-Series Measurements.**

M. T. Murrell and S. J. Goldstein, Isotope and Nuclear Chemistry Division, Los Alamos National Laboratory, K. W. W. Sims, Woods Hole Oceanographic Institute, and E. L. Hardin, University of Arizona

Studies of disequilibria among the long-lived members of the  $^{238}\text{U}$  and  $^{235}\text{U}$  decay series in high- and low-temperature fluids will be described. Thermal ionization mass spectrometric measurements were used to address the basic mechanisms that produce U-series disequilibria and to help constrain the mobility and reactivity of geologic fluids in the Earth.

Magmatic fluids: We have determined precise  $^{238}\text{U}$ - $^{230}\text{Th}$ - $^{226}\text{Ra}$ ,  $^{235}\text{U}$ - $^{231}\text{Pa}$ , and Sm-Nd isotopic ratios and concentrations in a series of systematic lavas from Hawaii which have trace-element and petrological characteristics indicating that they span a large range of melt fraction. Based upon this work, we find that the observed parent-daughter fractionations in Hawaiian basalts are primary magmatic features, which can be modeled in terms of melting of a garnet peridotite source with total melt fractions of 0.75% to 14%. These data also provide reasonable estimates of porosity (about 4%, independent of basalt type), melting rate ( $3 \times 10^3 \text{ kg/m}^3/\text{y}$  for tholeiites and  $7 \times 10^3 \text{ kg/m}^3/\text{y}$  for basanite), and melt velocity in the melting zone beneath Hawaii. A similar approach for mid-ocean ridge basalts indicates the MORB petrogenesis is qualitatively different from the Hawaii lavas with a wide range of porosities and a narrower range of melting rates.

Aqueous fluids: In an effort to investigate the nature of high  $^{234}\text{U}/^{238}\text{U}$  activity ratios commonly observed in perched waters associated with silicic tufts, we have analyzed samples from the Apache Leap Tuff near Superior, Arizona. Samples were obtained along a generalized flow path including an ephemeral stream, fracture zones near the surface, matrix pore water, a perched aquifer, and at a point where the aquifer discharges into a mine tunnel.  $^{234}\text{U}/^{238}\text{U}$  activity ratios in the surface and near surface waters range from 1.4 to about 2, while vadose zone pore water and perched waters show higher ratios which range from 4 to about 6.2. These differences in  $^{234}\text{U}$  fractionation can be modeled in terms of two mechanisms -- selective leaching of  $^{234}\text{U}$  and direct recoil of  $^{234}\text{U}$  into solution. Based on the short residence times and relationship between U concentration and the activity ratio, the dominant mechanism near the surface is selective leaching. Conversely, direct recoil appears to contribute significantly to the pore waters and perched waters. Ultimately, such data can be used to evaluate the transport of natural uranium in situations analogous to those proposed for the long-term geologic storage of radioactive waste.

## **Thermochemistry of Carbonates.**

A. Navrotsky, Department of Geological and Geophysical Sciences, Princeton University

High temperature oxide melt drop-solution calorimetric techniques have been developed and applied to carbonates in the  $\text{MgCO}_3$ - $\text{CaCO}_3$ - $\text{FeCO}_3$  system. Thermochemical data for carbonate-silicate equilibria involving magnesite-enstatite, calcite-wollastonite, and dolomite-diopside were used to check the consistency of the technique. The enthalpy of formation of siderite was determined directly and used to calculate equilibria in the Fe-C-O system. Ca-rich dolomites are energetically strongly destabilized and almost certainly represent metastable phases. Calorimetric studies along the  $\text{MgCa}(\text{CO}_3)\text{-FeCa}(\text{CO}_3)_2$  join show that the enthalpies of disordering of ankerites are much smaller than that of dolomite, and these energetics are consistent with the nonexistence of an ordered iron end-member. The energetics of mixing along the disordered  $\text{CaCO}_3$ - $\text{FeCO}_3$  join show significant positive heats of mixing, while the  $\text{MgCO}_3$ - $\text{FeCO}_3$  join is almost ideal. These data allow better understanding of sedimentation, diagenesis, carbonate dissolution, and the formation of dolomite.

Calorimetry of  $\text{SrCO}_3$ - $\text{CaCO}_3$  aragonite solid solutions shows significant positive heats of mixing in accord with electrochemical studies of Casey et al. The data suggest only a very small solubility of Sr in calcium carbonate and are relevant to problems of transport of radioactive and other pollutants.

## Recent Thermodynamic and Transport Property Measurements for Various Aqueous Geochemical Systems.

J. A. Rard and D. G. Miller, Earth Sciences Division and Chemistry and Materials Science Department, University of California, Lawrence Livermore National Laboratory

Isopiestic measurements were performed for  $\text{CaCl}_2(\text{aq})$  from 1.7682 to 10.253 mol/kg at 298.15 K with emphasis on high concentrations and supersaturated molalities. Literature data for the thermodynamic activities of  $\text{CaCl}_2(\text{aq})$  were critically evaluated and combined with the present results to yield the parameters of an extended version of Pitzer's model that is reliable essentially to experimental accuracy. It was necessary to include  $\text{CaCl}^+(\text{aq})$  ion-pairs in the analysis, but, unfortunately, published stability constant measurements do not yield a unique value for its formation constant.

Isopiestic measurements have also been made at 298.15 K for  $(\chi\text{H}_2\text{SO}_4 + (1 - \chi)\text{MgSO}_4(\text{aq}))$  over the molality range of about 0.9 to 9.5 mol/kg at  $\text{H}_2\text{SO}_4(\text{aq})$  molality fractions of  $\mathbf{c} = 6/7, 5/7$ , and  $4/7$ , which corresponds to the stoichiometric ionic strengths of  $I_s = 2.8$  to 32 mol/kg. The stoichiometric osmotic coefficients  $\mathbf{f}_s$  of  $(\mathbf{c}\text{H}_2\text{SO}_4 + (1 - \mathbf{c})\text{MgSO}_4)(\text{aq})$  show a regular decrease from  $\mathbf{c} = 1$  to  $\mathbf{c} = 0$  up to  $I_s = 18$  mol/kg, but at higher ionic strengths values of  $\mathbf{f}$  for the mixtures gradually increase above those for pure  $\text{H}_2\text{SO}_4(\text{aq})$ . Similar measurements were also made for the limiting binary solutions  $\text{H}_2\text{SO}_4(\text{aq})$  from 0.27470 to 0.70512 mol/kg and  $\text{MgSO}_4(\text{aq})$  from 0.50502 to 1.3080 mol/kg, where previous data are somewhat discordant.

Mutual-diffusion coefficients have been determined at 298.15 K for  $\text{K}_2\text{SO}_4(\text{aq})$  from 0.0050 to 0.5965 mol/dm<sup>3</sup> (near saturation), for  $\text{HCl}(\text{aq})$  from 0.1 to 12 mol/dm<sup>3</sup>, and for  $(\mathbf{c}\text{NaCl} + (1 - \mathbf{c})\text{Na}_2\text{SO}_4(\text{aq}))$  where  $\mathbf{c} = 1, 0.90, 0.75, 0.50, 0.25$ , and 0 at 0.5 mol/dm<sup>3</sup> using optical interferometry. These ternary solution measurements also yield the trace diffusion coefficients of  $\text{Cl}^-$  in  $\text{Na}_2\text{SO}_4(\text{aq})$  and of  $\text{SO}_4^{2-}$  in  $\text{NaCl}(\text{aq})$ . These experiments were done in collaboration with John G. Albright (Texas Christian University) and, for  $\text{HCl}$ , with Paola Rizzo (University of Naples).

Mixing rules (generalized Young's rules) have been examined for the densities and specific conductivities of ternary electrolyte solutions in terms of binary solutions values. Certain "natural" concentration and composition fractions were identified which yield the simplest mixing rules.

This research was supported under the auspices of the Office of Basic Energy Sciences (Geosciences) of the U.S. Department of Energy by the Lawrence Livermore National Laboratory under contract No. W-7405-ENG-48.

### **Stable Isotope Studies by Ion Microprobe.**

L. R. Riciputi, D. R- Cole, B. A. Paterson, and R. L. Ripperdan, Oak Ridge National Laboratory; H. Machel, University of Alberta, Canada; B. Pottorf and L. Summa, Exxon Production Research; J. Hendry, Queens University, Ireland; A. Boyce, Scottish Universities Research and Reactor Centre; and D. Crowe and S. Benezek, University of Georgia

The record of fluid-rock interactions, particularly at low and intermediate temperatures, is commonly preserved only at the microscale. Recent advances in ion microprobe techniques have led to an ability to investigate fluid-rock interactions at previously inaccessible scales, with precision that is sufficient to study a variety of isotopic processes in both natural and experimental systems. Results of ongoing investigations into the behavior of sulfur isotopes during burial diagenesis will be discussed, as well as initial results of combined oxygen isotope/trace element investigations into fluid/rock interactions that illustrate the potential of the ion microprobe.

The results of  $^{34}\text{S}/^{32}\text{S}$  analyses of Fe-sulfides from Upper Devonian carbonate reservoir rocks in the Western Canada Sedimentary Basin, Jurassic-Cretaceous sandstone reservoir rocks in the North Sea, and other diagenetic settings indicate that large variations ( $>50\%$ ) in  $\delta^{34}\text{S}$  values at the microscale (10's-1000's  $\mu\text{m}$ ) may be the norm rather than the exception. Two fields in Alberta, Canada, have been studied: the Nisky field (at the transition from sweet to sour gas) and the more deeply buried sour gas Obed field. Sulfide  $\delta^{34}\text{S}$  values from both fields display a bimodal distribution, with one maxima at  $-20$  to  $-15\%$ , and the other at  $+10$  to  $+20\%$ ; a  $50\%$  range in  $\delta^{34}\text{S}$  values is often recorded in single thin-sections. Multiple generations of sulfide can be identified, but essentially all sulfide formed during or after pervasive dolomitization, at burial depths  $>300$  m. The isotopic composition is generally correlated with sulfide paragenesis: sulfides formed during relatively shallow burial (300 to 1000 m) are typically light, whereas sulfides that are paragenetically related to carbonates formed during deep burial (3 to 5 km) are heavy. These distributions are consistent with two mechanisms of sulfate reduction - bacterial and thermochemical sulfate reduction. The results indicate that bacterial sulfate reduction persisted to depths deeper than typically encountered in shale diagenesis. Sulfide formation in these carbonate rocks is probably associated with different fluid events that supplied concentrations of iron, organic material, and possibly sulfate to the site of mineral deposition. Textural relations between pyrite, marcasite, and sulfate indicate that, although sulfide formation may be related to large-scale fluid events, most reactions were strongly influenced by local variations in microenvironments.

Although preliminary results from the North Sea indicate that the relation between paragenesis and isotopic composition is more complicated than in the Canadian rocks, there are many shared characteristics. Wide ranges in  $\delta^{34}\text{S}$  values are commonly observed at the thin-section scale (over  $100\%$  in some North Sea samples). Marcasite is abundant in both areas, and sulfide aggregates containing both marcasite and pyrite tend to have particularly variable  $\delta^{34}\text{S}$  values at the  $100\text{ }\mu\text{m}$  scale. Formation of the sulfides occurred relatively late during diagenesis, at burial depths of at least a few 100's of meters. Sulfide formation events appear to be related to regional fluid-flow occurrences, which served to supply necessary iron and organic material to the rocks.

A combined  $\delta^{18}\text{O}$  and trace element study of zoned garnets from the Dalnagorsk, Russia, boron deposit illustrates both the potential for analyzing  $^{18}\text{O}/^{16}\text{O}$  ratios in chemically variable phases and the ion microprobe's unique capabilities for both elemental and isotopic work.  $\delta^{18}\text{O}$  values vary by up to  $15\%$  in single garnets, and fluctuate over scales of  $<100\text{ }\mu\text{m}$ . Variations in isotopic composition are correlated with variations in trace (and major) element variations in the garnets, with high  $\delta^{18}\text{O}$  values associated with elevated B, Pb, LREE, and Fe contents. Isotopic



compositions are also correlated with sample location; deep samples located near the pluton have predominately high  $\delta^{18}\text{O}$  values (0 to +6‰), whereas samples located at shallow levels and on the flanks of the deposit range to much lower values (-5 to -15‰). The correlation of isotopic and element composition is consistent with a model of mixing of magmatic and meteoric water during formation of the deposit, with the boron (and most other trace elements) being sourced from the pluton.

## **Fluid and Heat Flow in the Gulf of Mexico Basin, South Texas.**

J. M Sharp, Jr., Department of Geological Sciences, The University of Texas at Austin

Fluid flow in the Gulf of Mexico Basin is characterized by the geopressured zone where flow rates are low but where concentrated zones or periods of fluid discharge are present. These are best documented by mineralogical, geochemical, and thermal patterns in the sediments. In shallower, basin margin areas, the meteoric system dominates. Deeper in the basin, the possibility of free convection (even in low-permeability sediments) is suggested both by theoretical models and by diagenetic and water chemistry data. A shale permeability of  $10^{-14}$  to  $10^{-17}$  m<sup>2</sup> is suggested by these models. Heat flow is dominated by conduction, but convection is also significant along some fault-zone systems. This includes the Wilcox Fault zone, which may represent a regional discharge area from the geopressured zone. Thermal conductivity and petrographic data for sandstones are presented for verifying mechanistic models of thermal conductivity. Thermal conductivity ranges from 2.0 to 5.75 W/m/K over a porosity range of 2-30%. At a given porosity, more quartzose sandstones are more conductive. A grain-matrix conductivity is adequately described with an arithmetic mixing model. The thermal conductivity of clean sandstone is a multilinear function of decreasing thermal conductivity with increasing porosity and increasing thermal conductivity with quartz content. Sandstones are isotropic with respect to thermal conductivity. Radiogenic heat production data for both clastic and carbonate rocks are presented which demonstrate that this heat source should not be ignored because it can contribute up to 40% of the surface heat flow density in the Gulf Coast. The hydraulic and thermal properties of shales on a regional basis remain the major unknown parameters. Also unclear is the degree of fluid transfer from the underlying basement, which should be undergoing metamorphism. These are major uncertainties remaining in the development of reasonable models of flow and transport in the Gulf of Mexico and similar sedimentary basins.

## **Case Studies of Stable Isotopes in Igneous Petrology.**

E. Stolper, S. Epstein, J. Eiler, and S. Nadeau, Division of Geological and Planetary Science, California Institute of Technology

This project integrates experimental studies of C-O-H volatile components in melts and glasses and field-oriented studies of specific petrological and volcanological problems. A key feature of this project is the combination of methodologies from stable isotope geochemistry and experimental petrology. Our results contribute quantitative constraints on the thermal and chemical evolution of specific magmatic systems and to a deeper understanding of the chemical and physical properties of volatile-bearing silicate melts and glasses. We present here three examples of our current work.

### Oxygen isotope fractionation between CO<sub>2</sub> vapor and felsic silicate glasses and melts:

Experimental studies to determine the fractionation of O isotopes between silicates provide constraints on interpretations of their distributions in natural systems. There have been few measurements of fractionation factors involving silicate melts or glasses, even though knowledge of such fractionations is necessary for understanding the behavior of O isotopes during igneous processes. We have measured the partitioning of O isotopes between CO<sub>2</sub> vapor and rhyolitic glass and melt, albitic glass, melt, and crystals, silica glass, and quartz. Our results show that the fractionation of oxygen isotopes between CO<sub>2</sub> and rhyolitic glass/melt can be modeled as a linear combination of our results on silica glass and albitic glass/melt, weighted according to the normative amounts of feldspar and quartz in the rhyolite. This demonstrates that the behavior of O isotopes in complex natural silicate melts can be understood by simple mixing of end member compositions, suggesting that a coherent basis for understanding the behavior of O isotopes in magmatic systems can be constructed with a finite number of experiments on the most important end members.

D/H ratios in apatite: Apatite is widespread in igneous, metamorphic, and sedimentary rocks. It is also unique among widespread minerals in that it contains non-negligible quantities of O, H, and C, and thus allows three of the major stable isotope systems to be investigated in a single mineral. We have measured H<sub>2</sub>O and CO<sub>2</sub> contents and D/H and <sup>13</sup>C/<sup>12</sup>C ratios of a range of natural apatites. This project has proven to be surprisingly challenging because, even after heating to 1500°C for >30 hours, natural apatites do not devolatilize fully unless the grain size is ≤100 μm; even for smaller grain sizes, heating must be done for several hours. However, a successful procedure has been developed that yields reliable results with minimal blank corrections. Most of our development effort has focused on apatites from carbonatites. δD<sub>smow</sub> for eleven apatites (0.5-1.1 wt % H<sub>2</sub>O) from four carbonatites are all ~-70‰, within the range of typical mantle values. The similarity to mantle δD values and the lack of correlation with total H<sub>2</sub>O content contrasts with the expected behavior of altered or exchanged minerals and suggests that apatite can preserve primary igneous δD values. The difficulty we experienced in getting the water out of the apatites is consistent with this inference that D/H ratios in apatites are difficult to exchange, and we conclude that this phase has the potential to provide insights into D/H ratios of magmas.

Oxygen isotopes in lavas from the Hawaii Scientific Drilling Project: In connection with the Hawaii Scientific Drilling Project and in collaboration with John Valley (University of Wisconsin), we used laser fluorination to measure δ<sup>18</sup>O in olivine phenocrysts from Hawaiian volcanoes and demonstrated for the first time significant correlations between δ<sup>18</sup>O and radiogenic isotopes. Results suggest a three-component mixing model, with a low <sup>18</sup>O component likely being the Pacific oceanic crust beneath the Hawaiian Islands. We also measured δ<sup>18</sup>O of olivines from ocean island basalts spanning the range of distinct mantle reservoirs to search for

variable  $\delta^{18}\text{O}$  reservoirs in the mantle. We identified several correlations between  $\delta^{18}\text{O}$  and radiogenic isotope ratios. For example, EM2 basalts are enriched in  $^{18}\text{O}$  relative to normal upper mantle, consistent with the presence of subducted sediment in their sources;  $^{87}\text{Sr}/^{86}\text{Sr}$  is positively correlated with  $\delta^{18}\text{O}$  among all ocean island basalts, and HIMU lavas and lavas with low  $^3\text{H}/^4\text{He}$  are often depleted in  $^{18}\text{O}$  relative to normal upper mantle, consistent with a component of recycled lower oceanic crust.

## **Geochemical Evidence for Fluid Flow in Carbonate Platforms.**

P K Swart., L Melim, and G Eberli, Marine Geology and Geophysics, University of Miami

Modern concepts of carbonate alteration are heavily biased by studies of shallow-water Pleistocene to recent sediments. As a result, these models are strongly influenced by the large changes in sea level which occurred during the Pleistocene. Recent evidence, however, suggests that significant alteration takes place in the subsurface of carbonate accumulations which have never been affected by sub-aerial processes. Such evidence occurs in the form of petrographic fabrics which are traditionally considered to be a result of meteoric diagenesis, yet which have occurred in zones, based on geochemical criteria such as stable carbon and oxygen isotopes, that have never been subjected to meteoric fluids. Such regions typically also have experienced extensive recrystallization as evidenced by the conversion from metastable minerals such as aragonite and high-Mg calcite to low-Mg calcite and dolomite. In addition, minerals such as celestite ( $\text{SrSO}_4$ ) are common. The formation of significant quantities of dolomite and celestite necessitates the movement of large amounts of fluid containing the necessary cations and anions. As local supply and the process of diffusion are simply insufficient, the presence of this alteration presents indirect evidence of subsurface movement of fluids.

In addition to such indirect evidence of fluid movement, direct observations of fluid chemistry and temperature have been obtained from several sites drilled by the Ocean Drilling Program and the Bahamas Drilling Project. Chemical analyses of fluids squeezed from sediments and temperature measurements obtained during drilling provide information on the nature of the geochemical profiles. Fluid movement out of the formation is characterized by concave upward profiles for both temperature and fluid chemistry, while fluid movement into the formation is characterized by the reverse pattern. The  $^{87}\text{Sr}/^{86}\text{Sr}$  ratio of the formation fluids relative to the same ratio of the host rocks can also indicate the presence of fluids suggestive of large-scale fluid movement. The best examples of these processes are shown in data obtained from Leg 133 of the Ocean Drilling Program. Site 812 was drilled into a submerged carbonate platform known as the Queensland Plateau. In spite of extensive recrystallization, there was very little change in the concentration of elements such as Sr which normally indicate recrystallization. In addition, the Sr-isotopic composition of the fluids was considerably more radiogenic than the host sediments. The  $^{87}\text{Sr}/^{86}\text{Sr}$  ratio combined with the Sr concentration gradient precludes the diffusion of modern Sr into the sediments and instead suggests lateral movement of waters through the formation. Temperature measurements obtained after drilling also suggested the presence of substantial amounts of under pressure in the sediments.

Similar evidence of exotic aquifers was obtained during the drilling of Leg 101 in the Bahamas. Several holes drilled into Exuma Sound exhibited non-steady state geochemical profiles, with anomalous porewater  $^{87}\text{Sr}/^{86}\text{Sr}$  ratios. The high  $\delta\text{D}$  and  $\delta^{18}\text{O}$  of the porewaters suggest a near surface origin for these fluids.

Mechanisms that may be responsible for such fluid movements have been investigated in conjunction with J. Bahr (University of Wisconsin). Basic input into the model has been obtained from seismic sections across The Bahamas in conjunction with permeability and porosity measurements made on samples obtained from two deep core borings. These models suggest that significant fluid flow takes place in the subsurface driven by the temperature differences between the platform interior and the adjacent seaways.

## Development of $^{81}\text{Kr}$ and $^{85}\text{Kr}$ Analyses for Use as Groundwater Tracers.

N. Thonnard, Institute for Rare Isotope Measurements, and L. D. McKay, Department of Geological Sciences, The University of Tennessee at Knoxville

The rare noble gas radioisotopes  $^{81}\text{Kr}$  and  $^{85}\text{Kr}$ , with 210,000 and 10.76 year half-lives, respectively, and  $\sim 10^{-12}$  isotopic abundance and  $\sim 10^{-22}$  concentration in modern water, have the potential to be very useful as groundwater tracers for determining groundwater ages, infiltration rates, and preferential flow paths for both local- and regional-scale flow systems.

$^{81}\text{Kr}$  has the potential of becoming a useful research tool for the dating of old groundwaters (10s to 100s of thousand years) for which there are relatively few age-dating methods available.  $^{81}\text{Kr}$  is well suited for dating of old groundwater because it is essentially nonreactive in the subsurface, has no known subsurface sources, has the appropriate half-life, and has had a relatively constant level in the atmosphere and in precipitation due to its cosmogenic origin and long atmospheric residence time.

$^{85}\text{Kr}$  is expected to have a wide range of applications in shallow, relatively young (<30 years) groundwaters and has several major advantages over other tracers (i.e.,  $^3\text{H}$ ,  $^3\text{He}$ , and CFCs). The principal advantages are that  $^{85}\text{Kr}$  is essentially nonreactive and its activity in the atmosphere, and hence in precipitation, has been continually increasing in the atmosphere due to mainly the nuclear fuel cycle. The average  $^{85}\text{Kr}$  input function for North America is well known and does not display the large "bomb peaks" characteristic of  $^3\text{H}$  inputs to groundwater. As well, because  $^{85}\text{Kr}$  is not present in typical industrial contaminants, it can be used in contaminated groundwaters where CFCs are unreliable. Age-dating with  $^{85}\text{Kr}$  is attractive because of its simplicity and reliability.

To date, only  $^{85}\text{Kr}$  has been applied to a very few test cases, and its full range of usefulness has not been investigated. This is partly because the only existing analytical method, decay counting, requires large water samples (20 liters, at best), and there are only two laboratories worldwide equipped to make them. The only  $^{81}\text{Kr}$  measurements from natural samples are a handful of results from old groundwater and polar ice using the proof-of-principle laser-based mass spectrometric system currently under development. (Decay counting would, in principle, require 20 million liters of water!)

This new technique, when fully operational at the Institute for Rare Isotope Measurements, should permit  $^{85}\text{Kr}$  measurements using only 1- to ~5-liter samples and  $^{81}\text{Kr}$  measurements from 10- to 20-liter samples. The technique presently consists of a multi-step process starting with (1) degassing of the sample, (2) separating Kr from the remainder of the gas, (3) a first isotopic enrichment, reducing interfering isotopes by  $10^5$ , (4) a second isotopic enrichment of  $10^3$ , and (5) detecting the rare krypton isotope in a time-of-flight mass spectrometer utilizing resonance ionization. As there are only a few thousand analyte atoms in the sample, the sensitivity, element selectivity, and immunity to interferences of resonance ionization is required. A detection limit of  $\sim 100$   $^{85}\text{Kr}$  atoms had been demonstrated earlier in the final mass spectrometer. Work in progress, which will make the system a practical analytical tool, includes characterization of the efficiency, accuracy, and blank level of each step, stabilization and automation of operating parameters in steps (1), (2), and (3), complete redesign of step (4), and improvement to the laser and data acquisition systems in step (5).

The next phase of research, scheduled to start this summer, involves development and testing of new sampling techniques (such as *in situ* degassing of the groundwater) and application of the  $^{85}\text{Kr}$  age-dating method to groundwater in a shallow, unconfined aquifer near Sturgeon Falls, Ontario, where it can be compared to existing groundwater age-dating methods.

**Scientific Cooperation with Russian Scientists on Contaminant Transport.**  
C-F Tsang, Earth Sciences Division, Lawrence Berkeley National Laboratory

The project provided a mechanism to invite research scientists and engineers in Russian research institutes to work in the U.S. for a short period of time (about one to three months) to interact with U.S. scientists and perform cooperative studies in the field of environmental contaminant transport evaluation and remediation. The purposes were

- to develop mutual scientific understanding and working relationship,
- to compare scientific experiences and approaches,
- to formulate collaborative projects based on each other's strengths, and - to jointly develop site characterization methods and predictive modeling methods for contaminant transport.

Over the last three years, thirteen Russian scientists were selected on recommendations from the Russian Academy of Sciences and the Russian Ministry of Atomic Energy, based on the individual's scientific experiences and activities. They were invited to work at the Lawrence Berkeley National Laboratory normally for a period of one to three months to give seminars, which were summarized in reports in English, to interact with U.S. scientists and engineers, and to develop plans for collaborative research projects. The invitees were all active scientists or engineers and were, to different degrees, able to communicate in English.

Out of these visits, the following has been accomplished:

- Twelve scientific reports have been published, with half of them already submitted to U.S. refereed journals; another ten reports or so are under various stages of editing and review.
- Good collaborations were established, not only between the Russian scientists and Berkeley Laboratory scientists, but also between them and scientists from other national laboratories, universities, and U.S. companies. Furthermore, collaboration was also stimulated among the Russian Institutes themselves.
- A two-week joint field test at Chelyabinsk Mayak site in South Urals, Russia, was proposed, planned, and then successfully carried out under funding from DOE/EM-OTD to study transport of radioactive contaminant in surface and ground water over the last 40-50 years at that site. Two papers on the results of the field test have just been completed and submitted to refereed journals.

## **Contrasting Mechanisms of Fluid/Rock Exchange.**

J. W. Valley, Department of Geology and Geophysics, University of Wisconsin at Madison

The ion microprobe and laser probe are complementary techniques for oxygen isotope analysis in silicates, carbonates, and oxides. The capabilities of these techniques have recently undergone dramatic improvements in terms of sample size, spatial resolution, reliability, and accuracy. Improved standardization and refined techniques yield routine precision and accuracy of  $\pm 0.05$ - $0.10\%$  (1 sd) by laser at 0.5-1.0 mm spatial resolution. The ion probe achieves unrivaled spatial resolution (1-20  $\mu\text{m}$ ) at some expense in precision, which is largely dictated by counting statistics. New fast-counting systems (DT = 12-14 ns) allow routine precision of better than 1‰ (1 sd) in 20 minutes, and 0.4‰ is possible in 50 minutes. Ten individual spot analyses of a homogeneous diopside standard have yielded 1 sd = 0.36‰ (vs. 0.4 for theory) with an uncertainty in the mean of 0.11‰.

It is now possible to make true microscale studies of fluid/rock interaction and to test theoretical predictions of fluid flow and mineral exchange. Initial studies reveal evidence of complex superimposition of multiple events and processes in many igneous, metamorphic, and sedimentary environments and disprove many macroscale predictions based on bulk-mineral analysis. Stable isotope thermometry should not be applied in many rocks, but attention to microscale processes permits greater reliability in appropriate samples. Recrystallization, new mineral growth, and volume diffusion may all influence the  $\delta^{18}\text{O}$  of a rock and its constituent minerals.

The ability to perform microanalysis of stable isotope ratios reinforces the importance of time-tested procedures for looking at rocks, including hand lens and microscope, as well as newer forms of imaging.

Growth zoning of  $\delta^{18}\text{O}$  is common and has been documented in quartz overgrowths (St. Peter sandstone) and pelite garnets (Cordillera Darwin and Vermont), recording variable temperature and fluid conditions. Zoning will be partly or wholly erased by volume diffusion if metamorphic conditions are sufficiently hot and prolonged, or cause recrystallization. Heterogeneity or zoning caused during cooling may be concentric or complex depending on the relative importance of grain boundaries vs. other fast pathways such as cracks, micropores, and crystal defects. The timing of exsolution vs. blocking can be important. Analyses of magnetite and diopside in granulite facies marble, and magnetite in granitic gneiss (Adirondack Mountains), variably record evidence of closed system intermineral exchange during cooling, exchange with retrograde fluids, fast grain boundary diffusion, and cryptic pathways of intramineral exchange. Some diopsides and magnetites show concentric low  $\delta^{18}\text{O}$  rims, apparently formed through volume diffusion, consistent with experimentally determined diffusion coefficients at high  $P(\text{H}_2\text{O})$ . In contrast, TEM examination of cryptically zoned magnetites documents fast transport along crystal defects, some of which are replaced by 400 nm thick layers of phyllosilicates.

Laser analysis of quartz from a single outcrop of shallow, hydrothermally altered granite (Isle of Skye) shows homogeneity in some samples, but heterogeneity in others. Ion probe analysis confirms this and documents the mechanism of quartz-water exchange. Heterogeneous quartz grains are cut by healed microfractures with  $\delta^{18}\text{O}$  as low as -3‰ and gradients of up to 13‰ over 400  $\mu\text{m}$  into unfractured quartz. Microanalysis of the Bishop Tuff (Long Valley) shows similar complexity. Thus, fluid flow and exchange in this environment are heterogeneous; crack-controlled and anisotropic; and proceeds under disequilibrium conditions.



## **The Transport of U, Th, Ir, and Re in Oxidizing/Reducing Environments from the Continents to the Sea.**

G. J. Wasserburg and D. Porcelli, Division of Geological and Planetary Sciences, California Institute of Technology

The importance of particles and colloids for the transport of actinides from the continents to the ocean was investigated in the Baltic Sea and Kalix River drainage basin, which drains a mire-rich region of northern Sweden. 'Particles' were separated from waters using 0.45  $\mu\text{m}$  filters and ultrafiltration techniques were used to separate U in the 0.45  $\mu\text{m}$ -filtered water associated with colloids  $>10$  k daltons (including inorganic particles, humic acids, and other large organic molecules) from "dissolved" U (U in solution or associated with smaller colloids). It was found that colloids carry a substantial ( $>50\%$ ) fraction of the U throughout the Kalix River. Near the mouth of the Kalix River, where the waters are rich in organic matter derived from the mire region, 0.45  $\mu\text{m}$ -filtered water had 184 ng/kg U and  $\delta^{234}\text{U} = 900$ , and  $\sim 80\%$  of this U was associated with  $>10$  k dalton colloids. Within the Gulf of Bothnia, U in waters with low salinity ( $\sim 3.3\text{‰}$ ) could be explained by mixing of seawater with the "dissolved" U in the Kalix River, suggesting that it is this "dissolved" U that behaves conservatively, while riverine U associated with  $>20$  k dalton colloids is removed during estuarine mixing. The association of U with colloids therefore may be an important parameter in determining U estuarine behavior. However, a significant fraction of U ( $\sim 50\%$ ) in the Gulf of Bothnia is also associated with colloids, indicating a continuing association of U with colloids in brackish waters. At higher salinities ( $>6\text{‰}$ ) in the Baltic Sea,  $\sim 10\%$  of the U is associated with  $>10$  k dalton colloids, a smaller but still significant fraction of the total U.

Within the Kalix River basin, peat samples from mires have dry weight U concentrations of  $\sim 10^5$  times that of associated mire waters. This indicates that U is highly concentrated in the organic matrix under the reducing conditions in the mires. Although mire waters are enriched in  $^{234}\text{U}$  relative to the peats, these waters have low U concentrations ( $<20$  ng/kg) and  $^{234}\text{U}/^{238}\text{U}$  ratios comparable to the river. These waters are therefore not the primary source of the excess  $^{234}\text{U}$  in the river. The most likely source of excess  $^{234}\text{U}$  in this area is groundwater.

The suspended particulate load ( $>0.45$   $\mu\text{m}$  particles) were found to be important carriers of U in the Kalix River, accounting for 20% of the U discharged into the Baltic. This U is rapidly removed by sedimentation, and  $<1\%$  of the U within the Baltic was found in the  $>0.45$   $\mu\text{m}$  fraction. Particles in both the Kalix River and Baltic Sea were found to have U with  $\delta^{234}\text{U}$  substantially higher than the equilibrium value as expected for detrital particles, and can be explained as a mixture of U scavenged from the surrounding water ( $>70\%$ ) and detrital U. U and Fe concentrations correlate in the river particles, suggesting that the scavenging agent is Fe oxyhydroxides (which constitute up to 50% of the particles).

In conjunction with a student, A. Anbar, we have obtained a set of reliable results on the concentration of dissolved Ir in waters from the deep sea, surface waters, an estuarine environment, and rivers. A comparison of Ir in both oxidizing and reducing conditions also was made. Ir has the lowest concentration in waters of any stable element and was found to be nonconservative. It was found that  $C_{\text{Ir}} = 3 - 6 \times 10^8$  atoms/kg in seawater and  $C_{\text{Ir}} = (17 - 95) \times 10^8$  atoms/kg in rivers. The residence time of Ir in the oceans is about  $5 \times 10^3$  years. Ir is rapidly removed from inflowing river waters upon reaching the estuarine environment. In reducing conditions, such as anoxic basins, Ir is not removed but remains in solution over a 10-20 year time. With the improved techniques developed in this study, it now will be possible to carry out on a "routine basis" a full investigation of all the PGE as well as Re in the weathering and hydrologic cycle.

## Hydrogen-Electrode Potentiometric Studies of Aqueous Geochemical Processes.

D. J. Wesolowski, D. A. Palmer, and R. E. Mesmer, Chemical and Analytical Sciences Division, Oak Ridge National Laboratory

In this research, we make use of the unique capabilities of our high temperature, pH-measurement cells (0-295°C), vapor saturation pressure) in experimental studies of key aqueous reactions involving  $H^+$ . Funding for this project specifically includes support for visiting scientists, and nearly all of our current activities involve external collaborators. Conceptually, the cells are very simple, containing a pair of Teflon cups housing platinum electrodes, connected through a common head space and a porous Teflon liquid junction. The cell is then purged with hydrogen and brought to temperature. After equilibration each electrode responds perfectly Nernstianly, with their potential difference defined as  $\Delta E = -(RT/F)\ln(aH^+_{test}/aH^+_{ref}) + E_{lj}$ . If the test and reference solutions are fixed at constant ionic strength with a "swamping" inert electrolyte, the potential becomes a highly accurate measure of the hydrogen ion concentration of the test solution relative to the reference solution.

Because of the current interest in the role of organic acids in permeability development, alteration, and metal transport in sedimentary basins and waste disposal sites, we have hosted Dr. Richard M. Kettler of the University of Nebraska for several summers to study the dissociation constants of oxalic, malonic, succinic, and benzoic acids in 0.03 to 5.0 molal NaCl to temperatures of 225, 100, 200, and 250°C, respectively. Also, with Dr. Kettler and his student, Moira Ridley who spent a year with us, we are now examining the complexation of  $Al^{3+}$  and  $Cd^{2+}$  by the anions of these acids. Dr. Pascale Benezeth, a postdoctoral fellow from Toulouse, France, is investigating the hydrolysis and acetate complexation of  $Cd^{2+}$  in sodium triflate (a noncomplexing anion) solutions to 200°C. Dr. Scott A. Wood of the University of Idaho also visited and measured the association constants of Nd-acetate species in 0.1 molal NaCl brines to 250°C in order to improve the use of Nd/Sm and REE analyses in interpretation of diagenetic and fluid migration events in sedimentary and hydrothermal systems.

With Kettler and Ridley, we have also measured the association constants of  $Al(SO_4)^+$  and  $Al(SO_4)_2^-$  from 5 to 125°C in 0.1 and 1.0 molal NaCl solutions. Our preliminary results indicate a surprising major increase in the stability of both species at temperatures below 50°C. An extensive series of conventional gibbsite -  $Al(OH)_3$  - solubility measurements in 0.1 molal NaCl +  $NaHSO_4$  solutions at 50°C, two pH's, and five total sulfate concentrations quantitatively confirm the potentiometric results at this temperature. Also, the rate of dissolution of gibbsite at 5 °C was found to be more than an order of magnitude faster in NaCl +  $H_2SO_4$  solutions versus NaCl + HCl solutions of the same pH at 0.1 molal ionic strength. If confirmed, this increase in complex stability at low temperature has important ramifications for modeling diagenetic processes and the effects of acid rain and acid mine drainage.

Recently we have been employing these cells for the first ever studies of mineral solubility and surface sorption characteristics with continues, *in situ* monitoring at temperatures above 100°C, including the solubility of boehmite -  $AlOOH$  - in 0.03 to 5.0 molal NaCl brines to 250°C with Dr. Benezeth; measurement of the pH of zero net surface charge on rutile surfaces and modeling the surface charge distribution as a function of temperature, pH, and ionic strength, in collaboration with Dr. Michael L. Machesky of the Illinois State Water Survey; and measurements of the solubility of magnetite in NaCl brines with Dr. Ken-Ichiro Hayashi, on sabbatical leave from Tohoku University in Japan. One of our future goals is to apply such measurement in precisely quantifying the rates of dissolution and precipitation of minerals as a function of temperature, pH, ionic strength, and degree of under- or super-saturation.

## **Toward an Equation of State for Nonelectrolytes in Water.**

R. H. Wood., Department of Chemistry and Biochemistry, University of Delaware

In previous work for DOE, the volumes and heat capacities of a variety of nonelectrolytes from room temperature through the critical point at pressures near 28 MPa were measured. The equation-of-state of Shock, Helgeson, and Sverjensky is of the wrong form to accurately correlate these results. We have found a new equation for the infinite dilution partial molar volume based on the direct correlation function integral that yields reasonably good fits to all of the experimental data with only two adjustable parameters for each solute.

In order to make predictions of the volumes and heat capacities of organic compounds at temperatures up to 250°C, we have made measurements on the volumes and heat capacities of a series of organic compounds. Analysis of the volumes shows that a functional group decomposition is able to fit all of the experimental data with good accuracy so that we now can predict the volume at infinite dilution of any compound composed of  $\text{CH}_3$ ,  $\text{CH}_2$ ,  $\text{OH}$ ,  $\text{NH}_3$ ,  $\text{NH}_4^+$ ,  $\text{CO}_2^-$ , and  $\text{COOH}$  groups at temperatures from 25 to 250°C. We have analyzed the heat capacities of the alcohols in a similar fashion and found that functional group methods also work for heat capacities at temperatures to 250°C. Work on the heat capacities of the other functional groups is progressing.

## ATTENDEES

### **Larry M. Anovitz**

Oak Ridge National Laboratory  
P.O. Box 2008  
Building 4500S, MS-6110  
Oak Ridge, TN 37831-6110

### **Jean Bahr**

Department of Geology  
University of Wisconsin  
Madison, WI 53706

### **Chris Ballentine**

Dept. Geol. Sci.  
2534 C. C. Little Bldg.  
University of Michigan  
Ann Arbor, MI 48109-1063

### **Hubert L. Barnes**

Dept. Geosciences  
Pennsylvania State University  
University Park, PA 16802

### **David R. Bell**

Carnegie Inst. Washington  
Geophysical Laboratory  
5251 Broad Branch Road  
Washington, DC 20015-1305

### **Pascale Benezeth**

Oak Ridge National Laboratory  
P.O. Box 2008  
Building 4500S, MS-6110  
Oak Ridge, TN 37831-6110

### **Robert Berner**

Dept. of Geology & Geophysics  
Yale University  
New Haven, CT 06520-8109

### **James G. Blencoe**

Oak Ridge National Laboratory  
P.O. Box 2008  
Building 4500S, MS-6110  
Oak Ridge, TN 37831-6110

### **Robert J. Bodnar**

Dept. Geological Sciences  
Virginia Tech  
Blacksburg, VA 24061

### **Susan Brantley**

Dept. Geosciences  
Pennsylvania State University  
University Park, PA 16802

### **James Brennan**

Lawrence Livermore Nat'l Lab  
P.O. Box 808  
Livermore, CA 94550

### **William H. Casey**

Dept. Land, Air & Water Resources  
University of California  
Davis, CA 95616

### **Thure Cerling**

Dept. Geology and Geophysics  
University of Utah  
Salt Lake City, UT 84112

### **Robert N. Clayton**

Dept. Geophysical Sciences  
University of Chicago  
Chicago, IL 60637

### **M. Ford Cochran**

Dept. Geological Sciences  
University of Kentucky  
101 Slone Bldg.  
Lexington, KY 40506-0053

### **David R. Cole**

Oak Ridge National Laboratory  
P.O. Box 2008  
Building 4500S, MS-6110  
Oak Ridge, TN 37831-6110

### **Paula M. Davidson**

U. S. Dept. Energy  
ER-15, G-357, GTN  
19901 Germantown Road  
Germantown, MD 20874-1290

### **Donald J. DePaolo**

Lawrence Berkeley Laboratory  
University of California  
1 Cyclotron Road  
Berkeley, CA 94720

### **John Eiler**

170-25  
California Institute of Tech.  
Pasadena, CA 91125

### **R. Douglas Elmore**

School of Geology & Geophysics  
University of Oklahoma  
810 Sarkeys Energy Ctr, 100 E Boyd  
Norman, OK 73019-0628

**Michael H. Engle**  
School of Geology & Geophysics  
University of Oklahoma  
830 Van Vleet Oval  
Norman, OK 73019

**James P. Evans**  
Dept. Geology  
Utah State University  
Logan, UT 84322-4505

**Robert Glass**  
Geohydrology Department  
Sandia National Laboratory  
Albuquerque, NM 87185-1324

**Steven Goldstein**  
Los Alamos National Laboratory  
MS-K484  
Los Alamos, NM 87545

**Alex Halliday**  
Department of Geological Sciences  
University of Michigan  
Ann Arbor, MI 48109

**Gilbert Hanson**  
State University of New York  
Department of Earth & Space Sci.  
Stony Brook, NY 11794

**T. Mark Harrison**  
Department of Earth & Space Sci.  
University of Valifornia  
Los Angeles, CA 90024

**Ken-Ichiro Hayashi**  
Oak Ridge National Laboratory  
P.O. Box 2008  
Building 4500S, MS-6110  
Oak Ridge, TN 37831-6110

**James F. Hays**  
7245 Early's Road  
Warrenton, VA 22186  
(RETIRED)

**Grant Heiken**  
Los Alamos National Laboratory  
P.O. Box 1663  
Los Alamos, NM 87545

**Richard L. Hervig**  
Center for Solid State Science  
Arizona State University  
Tempe, AZ 85287-1704

**Juske Horita**  
Oak Ridge National Laboratory  
P.O. Box 2008  
Building 4500S, MS-6110  
Oak Ridge, TN 37831-6110

**Marie C. Johnson**  
Dept. Geography & Environmental  
Engineering  
United States Military Academy  
West Point, NY 10996

**David B. Joyce**  
Oak Ridge National Laboratory  
P.O. Box 2008  
Building 4500S, MS-6110  
Oak Ridge, TN 37831-6110

**B. Mack Kennedy**  
Lawrence Berkeley Laboratory  
1 Cyclotron Road  
Berkeley, CA 94720

**William C. Luth**  
U. S. Dept. Energy  
ER-15, G-357, GTN  
19901 Germantown Road  
Germantown, MD 20874-1290

**Larry McKay**  
University of Tennessee  
Dept. Geological Sciences  
306 Geology & Geography Bldg.  
Knoxville, TN 37996

**Kevin D. McKeegan**  
Dept. Earth and Space Sciences  
University of California  
Los Angeles, CA 90024

**Robert E. Mesmer**  
Oak Ridge National Laboratory  
P.O. Box 2008  
Building 4500S, MS-6110  
Oak Ridge, TN 37831-6110

**William J. Meyers**  
Dept. Earth and Space Sciences  
State University of New York  
at Stony Brook  
Stony Brook, NY 11794-2100

**Michael T. Murrell**  
Los Alamos National Laboratory  
Isotope and Nuclear Chemistry Div.  
Los Alamos, NM 87545

**Serge Nadeau**  
170-25 California Institute of Tech.  
Pasadena, CA 91125

**Alexandra Navrotsky**  
Princeton University  
Dept. Geological & Geophys. Sci.  
Guyot Hall  
Princeton, NJ 08554

**Donald A. Palmer**  
Oak Ridge National Laboratory  
P.O. Box 2008  
Building 4500S, MS-6110  
Oak Ridge, TN 37831-6110

**Carlo Pantano**  
Dept. Geosciences  
Pennsylvania State University  
University Park, PA 16802

**Donald Porcelli**  
Div. Geological & Planetary Sci.  
170-25  
California Institute of Tech.  
Pasadena, CA 91125

**Joseph A. Rard**  
Lawrence Livermore Nat'l Lab  
P.O. Box 808  
Livermore, CA 94550

**Robert Ripperdan**  
Oak Ridge National Laboratory  
P.O. Box 2008  
Building 4500S, MS-6110  
Oak Ridge, TN 37831-6110

**Lee R. Riciputi**  
Oak Ridge National Laboratory  
P.O. Box 2008  
Building 4500S, MS-6110  
Oak Ridge, TN 37831-6110

**Peter A. Rock**  
University of California, Davis  
College of Letters and Sciences  
Davis, CA 95616

**Frederick Ryerson**  
Lawrence Livermore Nat'l Lab  
P.O. Box 808  
Livermore, CA 94550

**Christian Schmidt**  
Dept. Geological Sciences  
Virginia Tech  
Blacksburg, VA 24061

**Mitch Schulte**  
Campus Box 11690  
Earth, Planet, Sci.  
Washington University  
St. Louis, MO 63130

**Jeffery C. Seitz**  
Oak Ridge National Laboratory  
P.O. Box 2008  
Building 4500S, MS-6110  
Oak Ridge, TN 37831-6110

**John M. Sharp, Jr.**  
Dept. Geological Sciences  
University of Texas  
P.O. Box 7909  
Austin, TX 78713-7909

**Edward Stolper**  
California Institute of Technology  
Division of Geological and  
Planetary Sci.  
Pasadena, CA 91125

**Peter K. Swart**  
MGG/RSMAS  
University of Miami  
Miami, FL 33149

**Norbert Thonnard**  
Institute Rare Isotope Measurements  
University of Tennessee  
10521 Research Dr. #300  
Knoxville, TN 37932

**Thomas Torgersen**  
University of Connecticut  
Dept. of Marine Sciences  
1084 Shennecossett Road  
Groton, CT 06340-6097

**Chin-Fu Tsang**  
Lawrence Berkeley Laboratory  
University of California  
1 Cyclotron Road  
Berkeley, CA 94720

**John Valley**  
Department of Geology  
University of Wisconsin  
1215 W. Dayton Street  
Madison, WI 53706

**Maxim Vityk**  
Dept. Geological Sciences  
Virginia Tech  
Blacksburg, VA 24061

**Gerald J. Wasserburg**  
California Inst. Technology  
Division of Geological and  
Planetary Sciences  
Pasadena, CA 91125

**David J. Wesolowski**  
Oak Ridge National Laboratory  
P. O. Box 2008  
Building 4500S, MS-6110  
Oak Ridge, TN 37831-6110

**Henry R. Westrich**  
Geochemistry Dept. 6118  
MS-0750  
Sandia National Laboratories  
Albuquerque, NM 87185-0750

**Robert H. Wood**  
Dept. Chemistry and Biochemistry  
University of Delaware  
Newark, DE 19716

**Nicholas B. Woodward**  
U. S. Dept. Energy  
ER-15, G-357, GTN  
19901 Germantown Road  
Germantown, MD 20874-1290